Some characteristics of infrared emitting diodes relevant to luminescence dating

N. A. Spooner and M. Franks
Research Laboratory for Archaeology and the History of Art, 6 Keble Road, Oxford, OX1 3QJ, UK

Introduction

Following the report by Hütt at the 1987 Cambridge TL Seminar (Hütt et al, 1988) that a dating signal could be obtained from K-feldspar using stimulation wavelengths of 860 nm and 930 nm, we investigated the use of an array of IR emitting diodes for this purpose. This paralleled work at Durham already reported (Poolton and Bailiff, 1989), and follows the success of Godfrey-Smith et al (1988) in exciting luminescence from feldspars by such a diode. Although various sources of IR radiation have been applied - for example, Hütt et al in their original work used a xenon lamp and monochromator, and later (Hütt and Jaek, 1990) an excimer dye laser and IR diode laser - the utilization of IR LED's appears attractive for reasons of economy, safety and convenience.

Trials of a simple IR LED set based on an array of twelve 880 nm diodes (TEMT 8850) showed a substantial fall in output intensity during the minutes after switch-on, the percentage difference between the initial and stable levels increasing with current. Similar behaviour has been reported by Poolton and Bailiff (1989) for an array of 16 Telefunken TSUS 5402 diodes. This suggested the need for "photofeedback control" if a constant intensity beam was to be maintained. To this end, a 1cm "large area" silicon photodiode was incorporated into the unit (peak response of 0.5A/W at 900 nm, diminishing to 5% of peak response at 350 nm and 1150 nm). While this approach was very successful for short exposures (<1 s), it proved unable to control satisfactorily the output beam for extended exposures (>1 s). Following verification that the photodiode and associated circuitry performed correctly, it was established that the failure to control resulted from a drift in the output spectrum of these IR diodes of ~10 nm, to longer wavelengths, which when coupled to the wavelength dependent response of the photodiode meant that although the photodiode output was held constant, the LED output was not. This occasioned a comprehensive investigation of IR LED characteristics, as reported in the next section. Brief details of the unit that was subsequently developed and some aspects of its performance are given in the final sections.

IR LED characteristics

The spectral dependence of the responsivity of suitable controlling photodiodes made it appear necessary for an LED type showing virtually no wavelength drift to be found. The "initial" output spectrum (2 seconds after switch on) and that after "stabilization" by 30 minutes continuous operation were therefore measured, using a silicon photodiode at the exit slit of an Oriel monochromator (model 7240). The set was calibrated using a sodium lamp, and the spectra corrected for detector response. The percentage reduction of radiant power and the magnitude of the shift to longer wavelengths was greater at higher currents in all cases, as is to be expected since the changes are dependent on LED junction temperature (eg Optics Guide 4, Melles Griot, 1988; GE/RCA Optoelectronics Data Book, 1987). Some examples of measured diode spectra are given in figure 1.

A significant difference between the behaviour of the resin bodied diodes and that of the metal encased diodes tested (see table 1) became apparent - the latter showed more severe intensity and wavelength shifts than resin-bodied types. Also, as a metal-encased diode requires electrical isolation from its neighbours (for series connection) this type was excluded from further study.

The output of unwanted, visible wavelength emissions was also considered. Emissions from arrays of 24 diodes each of types TSUS 5402 and TEMT 484 were measured by an EMI 9635Q PMT and 2 mm thick Schott BG 39 colour glass filter (passband 370 nm to 580 nm; 50% transmission) monitoring light scattered from a ground glass disc (25 mm diameter) placed on the TL oven plate. At a diode current of 50 mA, without the 12 mm diameter light guide and associated holder positioned, the TSUS 5402 array gave a countrate of ~150 cps above dark count, and the TEMT 484 gave ~100 cps. When the light guide and holder were emplaced both countrates dropped, to ~48 cps and ~10 cps respectively. The addition of a 4 mm thick Corning 7-59 filter (passband 320 nm to 430 nm; 50% transmission) reduced the countrate from the TSUS 5402 array to ~5 cps, but left the TEMT 484 array value unchanged. Given that the ground glass disc has about 2 - 4 times the reflectivity of a typical clean stainless steel disc, these levels were considered acceptable. It is assumed that visible wavelengths were involved but incomplete blockage of IR by the BG 39 cannot be ruled out.

The LED array

By operating the diodes at a low enough current for warm-up effects Poolton and Bailiff (1989) obtained satisfactory operation without feedback control. In our module we use higher currents but allow a warm-up time (typically 30 min) before measurements are commenced; sample illumination is actuated by means of a fast electronic shutter. A passive photodiode monitors the IR beam and permits manual control. An advantage of this arrangement is that, with shutter closed, the output current of the photodiode, being dependent on the detection of IR photons scattered from the shutter blades, avoids any effects due to variations in sample-to-sample reflectivity.

The LED chosen was TEMT 484 (for spectrum, see fig. 2). The narrow beam cone permits the array to be focused onto the sample from a sufficient distance to allow the shutter to be interposed, without losing power at the sample by beam spreading. The array is shown in figure 3, and further details may be found in Spooner et al (1990).

Performance

The unit is inserted in a standard TL set between the PMT and glow-oven, so making the TL oven available as a servo- controlled isothermal plate to maintain the sample temperature to within ~ ±1 °C; this is necessary because the initial sample luminescence increases by ~ 1 % / °C.

The run-to-run variation of beam intensity, as set manually from the monitoring photodiode reading and measured at the sample position by an on-plate photodiode arrangement is < 0.5% at 50 mA. Even without manual control long term stability is good - over 10 hours the beam intensity remained within ~ ±1 % of the intensity 1 hour after switch on. This was with the laboratory temperature held constant to ~ ±3 °C using an air conditioner.

The uniformity of sample illumination was checked by observing the luminescence stimulated by giving short IR exposures to a small chip of irradiated microcline feldspar positioned at various points on a sample disc (following Poolton and Bailiff, 1989). The intensity profile across a 9.7 mm disc was found to be circularly symmetric, with peak power at the central position dropping to 95 % at 3 mm distance and ~ 80% at the rim. Rotation of the module through 360° indicated a variation in total power delivered to the sample position of <0.5 %, as monitored by the on-plate photodiode (see fig. 4). The IR power received by the sample was 10.7 mW cm^{-2} at 50 mA; measured using the on-plate photodiode calibrated against a known power beam of 514.5 nm Ar-ion laser light, with due allowance being made for wavelength difference. In addition, qualitative observations of the IR beam were made using IR convertor cards, while a convenient check of the overall system performance is given by short-exposure monitoring of standardized portions of a bright, old sample, such as loess of several hundred thousand years age.

A single 2 mm Schott BG 39 is used as the basic optical filter required to shield the PMT from scattered IR photons (the unshielded EMI 9635Q tube detects ~105 cps from the above set, operated at 50 mA). Additional filters, such as Corning 7-59 or Schott GG-455 colour glass filters, may be added to this to select more specific detection wavebands. Leakage of IR onto the sample through the closed shutter was measured as $<10^{-6}$ of the beam power received by the sample with shutter open.

Summary

All types of LED tested showed output beam wavelength shifts and intensity decreases during warm-up; the wavelength shift precludes the use of a straightforward feedback control system based on a photodiode. Hence for our array we have chosen a type (TEMT 484) having a narrow beam which allows the diodes to be sufficiently far from the sample for an electronic shutter to be interposed; the diodes are kept on continuously and so deliver a stable output beam.

Acknowledgements

We gratefully thank D. Seeley for the mechanical fabrication of the apparatus, and A. Bowley for much of the electrical work. Valuable discussions with M. J. Aitken and B.W. Smith were also appreciated.

References

GE/RCA (1987) Optoelectronics Data Book

Hütt, G., Jaek, I. and Tchonka, J. Optical Dating : K-feldspars optical response stimulation spectrum. *Quat. Sci. Rev.*, **7**, 381-386 (1988),

Hütt, G. and Jaek, I. (1989) Infrared photoluminescence (PL) dating of sediments: modification of physical model, equipment and some dating results. In: Long and Short range limits in Luminescence dating, Occasional publication No. 9 of the Research Laboratory for Archaeology and the History of Art, 21 - 25.

Hütt, G. and Jaek, I. (1990) Photoluminescence dating on alkali feldspars: physical ground, equipment and some results. *Rad. Prot. Dosimetry.*, in press.

Optics Guide 4 (1988), Melles Griot.

Godfrey-Smith, D. I., Huntley, D. J. and Chen, W. H. (1988) Optical dating studies of quartz and feldspar sediment extracts. *Quat. Sci. Rev.*, **7**, 373-380.

Poolton, N. R. J. and Bailiff, I. K. (1989) The use of LEDs as an excitation source for photoluminescence dating of sediments, *Ancient TL*, **7**, 18-20.

Spooner, N.A., Aitken, M.J., Smith, B.W., Franks, M. and McElroy, C. (1990) Archaeological dating by infrared-stimulated luminescence using a diode array. *Rad. Prot. Dosimetry*, in press.

PR Ian Bailiff

Table 1. Characteristics of various IR LEDs.

Note Diode	Manufacturer	*1* Power	*1* Cone 1/2 angle	*1* Peak λ (nm)	Measured FWHM (nm)	*2* Spectral shift (nm)	*3* Spectral shift (nm)	*4* Int'y change Power	Temp. coeff's λ	Temp. coeff's	Comments
TEMT 8850	Three-Five Systems Ltd.	50 mW/SR at 100mA	15°	880	68	7	12	10.9	-	-	metal jacket
TEMT 484	Three-Five Systems Ltd.	100mW/SR at 100mA	8°	880	72	7	7	6	-0.53% per °C	-	resin
SFH 481-1	Siemens	10-20 mW/SR at 100mA	15°	880	86	8	14	14.3	-0.50% per °C	0.25 nm/°C	metal jacket
LED 55C	GE/RCA	5.4 mW at 100mA	15°	940	40	6	-	19.4	-	0.28 nm/°C	metal jacket
LED 55CF	GE/RCA	5.4 mW at 100mA	38°	940	40	7	-	15.5	-	0.28 nm/°C	metal jacket
CQX 19	Telefunken	20 mW at 250mA	40°	950	40	5	-	12	-	-	metal jacket (bulky)
TSUS 5402	Telefunken	15 mW at 100mA	25°	950	59	7	8	7.2	-0.80% per °C from 25°C	-	resin
IN 6266	GE/RCA	0.25 mW	20° at 100mA	940	40	5	-	11.6	-	0.28 nm/°C	metal jacket

Notes
1.Manufacturer's data
2.Shift in peak wavelength at 50 mA between 2 seconds and 30 minutes after switch on
3.Shift in peak wavelength at 100 mA between 2 seconds and 30 minutes after switch on
4.Intensity change at 50 mA between 2 seconds and 30 minutes

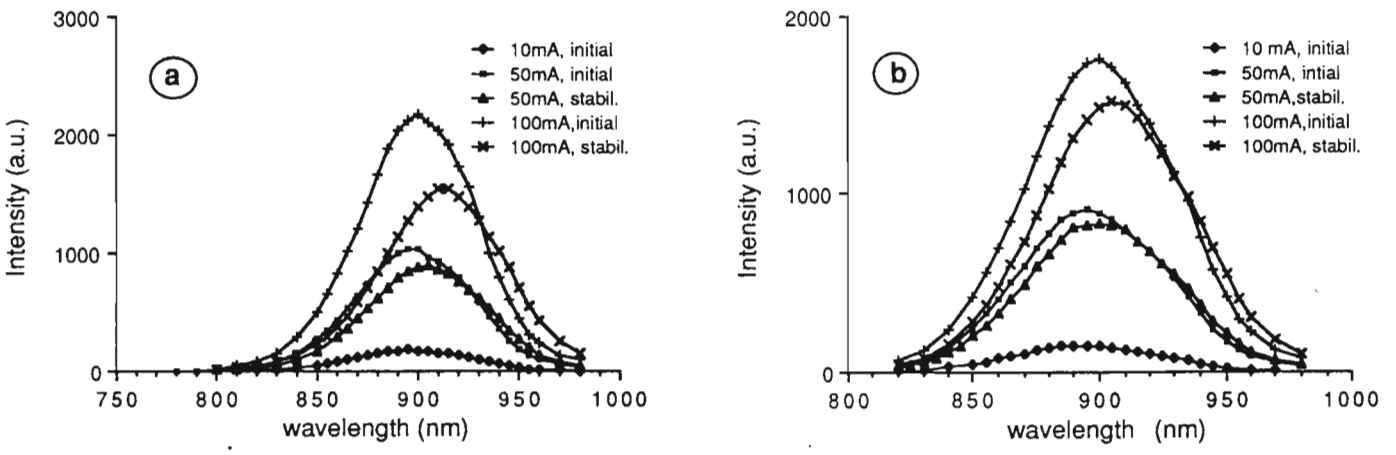

Figure 1.
The initial and stabilized output spectra of single (a) TEMT 8850 diode and (b) TEMT 484 diode, at 50 mA and 100 mA. Data taken following 30 minutes operation at 10 mA are also shown, and were indistinguishable from the initial output spectra at this current, within experimental error. Uncertainty in wavelength is within the data points. ("Initial" refers to measurements made 2 seconds after the diodes were switched on, and "stabilized" indicates 30 minutes continuous operation before measurement).

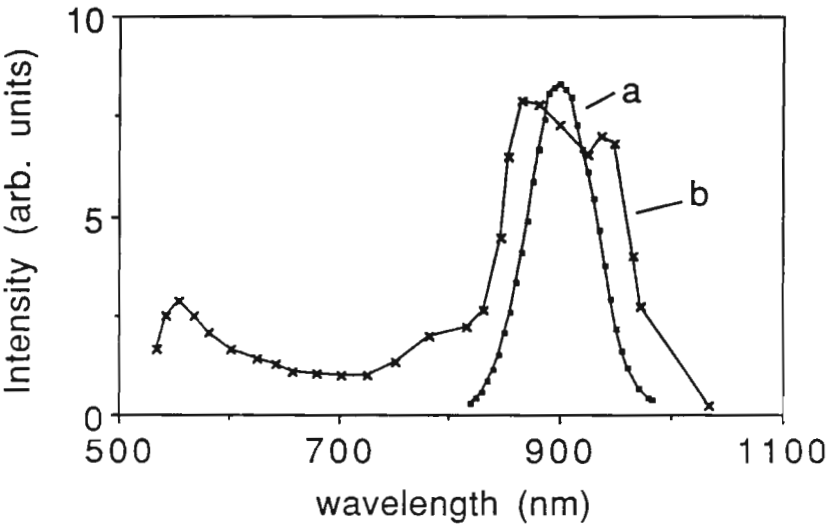

Figure 2
(a) The stabilized output spectrum of a single TEMT 484 diode operating at 50 mA.
(b) The optical response spectrum of alkali feldspar according to Hütt and Jaek (1989).

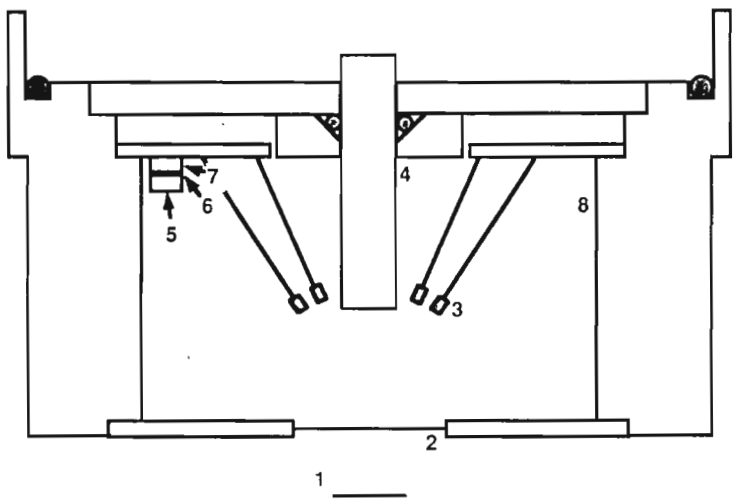

Figure 3
Schematic diagram showing the IR LED unit.
Components are: 1) sample, 2) 25.4 mm aperture Ilex electronic shutter, 3 ms full open or close time, Melles Griot, 3) diode array, 4) 12 mm diameter quartz light guide, 5) monitoring photodiode (Siemens IR-sensitive PIN photodiode, #BPW 34, temperature sensitivity ~0.05 %/°C), 6) monitoring thermo-couple, 7) Peltier effect heat pump, and 8) aluminium body.

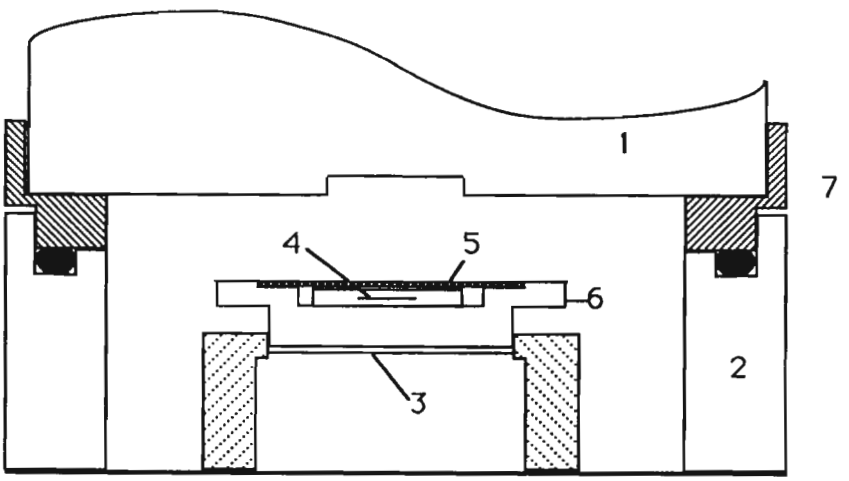

Figure 4
Schematic diagram showing the photodiode and filter assembly used for on-plate beam power calibrations and monitoring. The 1 cm^2 active area silicon photodiode presents a target area equivalent to that for a sample disc; flux reduction to levels giving linear photodiode response with power is achieved using 2 x 2.0 ND neutral density filters (Kodak and Schott).

1) LED array, 2) TL oven 3) oven plate, 4) photodiode, 5) filters, 6) X-Y spacer, 7) Z spacer.

Dose response of the paramagnetic centre at g = 2.0007 in corals

Rainer Grün
Subdept. of Quaternary Research, Cambridge University, Free School Lane, Cambridge CB2 3RS, UK.

In ESR dating, the accumulated dose AD is usually determined via the additive dose method (Aitken, 1985). In order to get reliable estimates of this parameter, the dose response has to be mathematically described and the results are then applied to the extrapolation procedure. In the early days of TL/ESR dating, it was often assumed that the sample was in "the linear part" of the dose response curve and hence linear fitting was applied. Apers et al. (1981) suggested an exponential fitting procedure by plotting $-\ln(1 - I/I_{max})$ versus the artificial dose (where I is the measured ESR signal intensity and I_{max} is the maximum ESR signal intensity when all traps are filled). As pointed out by Grün & Macdonald (1989), this procedure may lead to slightly erroneous results because the converted data may attain different weights. They also noted that the dose response of some samples cannot be described by a single exponential function and that a function with an additional exponent:

$$I = I_{max} (1 - \exp(-a(D-AD)^{\Gamma}))$$

may yield more satisfactory results (D = dose; a = fraction of unfilled defects that trap electrons per dose unit). It was subsequently emphasized by Levy (pers. comm.) that there is no physical reason for the additional exponent Γ.

During a dating study of corals from Huon Peninsula, New Guinea (where all ESR parameters were independently determined using other dating techniques) it was found that the application of a single exponential function led to systematic AD overestimations. AD assessments with an additional exponent of $\Gamma = 0.848$ did not yield "good agreement with U-series dating", but "good agreement with previous independent dating estimates" (Grün, 1990). Similar observations were also made in other laboratories (Barabas, pers. comm.).

In order to study this problem, 15 coral samples were collected from Holocene reef tracts in Kikai (Japan). Aliquots of 100 mg were irradiated in 12 steps with a calibrated gamma source and the paramagnetic centre at g = 2.0007 was recorded with a modulation amplitude of 0.05 mTpp and microwave power of 5 mW (JEOL RE1X ESR spectrometer). The ESR intensities are given in table 1. The sensitivities of the corals vary by about 50% and this may depend on the species. The AD's of all samples are well below 5 Gy, which corresponds to about 8,000 years for a surface sample. In order to eliminate individual effects and to force the dose response curve through zero (i.e. $I_0 = 0$), the natural intensity was subtracted from measured values, and subsequently normalized to the highest value (from sample 763: 686.1 Gy) and averaged. This averaged set (see table 2) was used for further statistical analysis, using the computer program FITT (Grün & Macdonald 1989). The fitting is based on the optimization of the sum of squares of the vertical distances of the data points from the calculated line SSQ.

When a single exponential function is applied to this data set, the AD increases systematically as more values are included in the regression procedure (see table 2). When using an optimization procedure for the additional exponent, the AD estimates are quite close to the expected value of zero. However, the exponent itself does not remain constant but changes systematically as more values are included. This leads to the conclusion that neither a single exponential function nor the "gamma-function" describe the dose response correctly.

Following the idea that the ESR signal at g = 2.0007 may be generated by two different paramagnetic centres, two exponential functions are optimized in the next step:

$$I = I_{max1} (1 - \exp(-a_1 (D - AD_1)) + I_{max2} (1 - \exp(-a_2 (D - AD_2))$$

First, both functions are forced through the origin (i.e. $AD_1 = AD_2 = 0$). This yields the following curve parameters:

$I_{max1} = 2660$; $a_1 = 0.0058$; $I_{max2} = 711800$;
$a_2 = 0.0000129$; SSQ = 16270

When additionally optimizing for AD_1 and AD_2 the results are:

$I_{max1} = 2747$; $a_1 = 0.005559$; $AD_1 = -1.25$
$I_{max2} = 708700$; $a_2 = 0.0000128$; $AD_2 = -0.15$;
SSQ = 15390

In order to assess the uncertainties of these values, a jackknifing procedure was used (see Grün & Macdonald 1989):

$I_{max1} = 2740 \pm 471$;
$a_1 = 0.005559 \pm 0.0011$; $AD_1 = -1.18 \pm 1.60$
$I_{max2} = 708700 \pm 86600$;
$a_2 = 0.0000128 \pm 0.0000009$; $AD_2 = -0.15 \pm 0.72$
SSQ = 15760

Both AD values are very close to zero. The second exponential function is nearly linear in the dose range investigated here and can be approximated by the following linear function (forced through $I_0 = 0$, see also Figure 1):

$$I = 9.15\ D$$

When this linear function is subtracted from the original data set (see Figure 1), the remaining data are best fitted by a single exponential function with:

$I_{max} = 2662$; $a = 0.0058$; $AD = -1.029$; SSQ = 15730

or, when forced though $I_0 = 0$ (see also fig. 1):

$I_{max} = 2656$; a = 0.005885; SSQ = 16370

Note that (1 - 1/e) I_{max} is already reached at 170 Gy. It can be seen that the latter two functions have very similar parameters to the first of the two exponential functions above.

The statistical analysis of the averaged data set suggests that the general dose response in the range of 0 to 700 Gy of the paramagnetic centre at g = 2.0007 in corals can be described by a linear and an exponential function. Because of the nearly linear part in the function set, it is not very likely that the ESR intensity at g = 2.0007 is generated by two paramagnetic centres. However, this type of dose response behavior can be expected when traps are created during irradiation (see Levy 1985; 1989) where:

$N = N_0 + K D$

(N = number of traps (or defects); N_0 = number of traps before irradiation). The dose response is then described by (see Figure 1):

$I = (N_0 - K/a) [1 - \exp(-aD)] + KD.$

Following from the results above we get:

$N_0 = 4211$; K= 9.15; f = 0.005885; SSQ = 16395

If the latter formula is applied for AD-determination it seems advantageous to use jackknifing for error assessment (Grün & Macdonald 1989).

The quality of the averaged data set is not sufficient to conclude whether the production of paramagnetic centres is best described by a single trapping scheme (single exponential function) or a more complex mechanism (Katzenberger & Willems, 1988).

The measurements of these Holocene corals strongly suggest that artificial irradiation causes the production of defects and this effect has to be considered when determining the accumulated dose.

Acknowledgements

This study was supported by SERC and by a grant of the "Wissenschaftsminister von Nordrhein-Westfalen (F.R.G.)" to U. Radtke. The field to Japan trip was supported by the DFG. I wish to thank Y. Ota, Yokoyama University, for her support and hospitality and U. Radtke, Universitt Dsseldorf, for his help in the field. I am grateful to P. Clay, Imperial College, London, for making the gamma source available.

References

Aitken, M.J. (1985) *Thermoluminescence dating*. Academic Press, London, 359.

Apers, D., Debuyst, R., DeCanniere, P., Dejehet, F. & Lombard, E. (1981) A criticism of the dating by electron paramagnetic resonance (ESR) of the stalagmitic floors of the Caune de l'Arago at Tautavel. In: DeLumley, H. & Labeyrie, J. (Hrsg) Absolute dating and isotope analysis in prehistory - methods and limits. Preprint, S., 533-550.

Grün, R. (1990) ESR-U-series comparisons, reefs II to IV.- Presentation at: International Workshop on Quaternary Sealevel Change, 15-21 March, 1990, Kikai, Japan.

Grün, R. & Macdonald, P.D.M. (1989) Non-linear fitting of TL/ESR dose response curves. Applied Radiation and Isotopes, 40(10-12), 1077-1080.

Katzenberger, O. & Willems, N. (1988) Interferences encountered in the determination of AD of mollusc samples. Quaternary Science Reviews, 7, 485-489.

Levy, P.W. (1985) Overview of nuclear radiation damage processes: phenomenological features of radiation damage in crystals and glasses. SPIE, 541, 2-24.

Levy. P.W. (1989) Principles determining the length of time material can be dated by TL, ESR and other trapped charge buildup methods. Seminar on Long and Short Range Limits in Luminescence Dating, Oxford, April 11-13, 1989. Research Laboratory for Archaeology and the History of Art Occasional Publication # 9, 33-38.

PR Reviewer's Comments (Anne F. Skinner)

There is little question that a major bottle-neck in the successful application of ESR to dating is the absence of a sound model that explains the complex observed phenomena. Any serious contribution to this effort is therefore welcome.

This paper, part of a longer presentation at a recent conference, puts forth evidence for such a model. In the absence of full discussion of dates before and after application of the model, the evaluation rests primarily on statistical grounds. There are three alternative mathematical approaches. On going from the first ("single exponential") to the second ("gamma factor"), the SSQ drops very significantly. However, when going to the third ("double exponential"), there is no further improvement in SSQ. Given that the last equation has six parameters, and the second only four, an improvement would be expected even if the double exponential equation was no better at modelling the system than the gamma-factor equation. Of course in both cases the AD parameters are constrained to zero, both in theory and in fact, so it is perhaps more accurate to suggest that one is going from a three-parameter equation to a four-parameter one. Nonetheless, considering only statistical factors, there is no overwhelming reason to favour the concept of a double exponential fitting equation. However, one must also consider that the double exponential equation may have some basis in physical reality, whereas the gamma-factor one does not. The reference by Levy puts forth some theoretical models, and the observed results in this paper match one of his suggestions. And it is certainly possible that defects are being created by radiation, rather than simply filled. There may, of course, also be other physical models that produce the same mathematical result (such as two overlapping traps with widely differing mean lifetimes). Overall, Dr. Grun has outlined an ingenious approach to data analysis. The evidence presented is suggestive of Levy's models, although not compelling, The results, one expects, will be very useful in stimulating discussion and suggesting other lines of investigation.

Table 1: ESR intensity of the signal g = 2.0007 [a.u.] normalized on 100 mg.

Dose [Gy]	763	764	765	766	767	768	769	770	771	772	773	774	775	776	777
0	63	62	57	45	24	30	25	58	49	54	29	64	50	65	48
10.7	337	331	244	214	262	263	270	336	254	236	223	315	325	374	243
21.4	593	560	415	388	468	476	474	594	454	395	422	541	569	631	432
42.9	1032	1020	795	683	865	854	866	1056	797	713	767	976	1029	1089	804
85.8	1917	1854	1408	1211	1603	1605	1607	1868	1495	1281	1415	1778	1845	1996	1441
171.5	3245	3215	2425	2170	2685	2785	2820	3145	2485	2245	2525	3060	3160	3490	2380
257.3	4395	4445	3420	2960	3665	3795	3835	4055	3330	2760	3450	4160	4225	4520	3230
343.0	5385	5390	4315	3595	4555	4765	4775	5065	4070	3825	4235	5060	5230	5730	3940
428.8	6325	6200	4980	4285	5310	5510	5460	6150	4445	4515	4940	5955	6205	6230	4670
514.6	7295	7160	5545	4855	5940	6125	6230	6670	5395	5060	5550	6710	7005	7280	5175
600.3	7995	7990	6265	5480	6750	7100	7150	7680	5855	5720	6305	7640	7925	8195	5900
686.1	8910	8645	6835	5915	7285	7685	7725	8195	6575	6230	7040	8345	8470	8820	6440

Table 2. Averaged data and fitting for the data up to the respective line.

Dose [Gy]	norm. average	exponential fitting AD [Gy]	SSQ	gamma-fitting gamma	AD[Gy]	SSQ
0	0					
10.7	275±18					
21.4	526±29					
42.9	993±42					
85.8	1873±83					
171.5	3234±88	- 0.1±0.3	289	1	- 0.1	289
257.3	4369±144	- 0.6±0.8	1903	0.954	0.1	963
343.0	5461±101	- 1.9±1.8	14671	0.891	0.6	5190
428.8	6422±152	- 2.9±2.1	25806	0.871	0.8	6135
514.6	7189±107	- 3.2±1.9	27654	0.891	0.5	7484
600.3	8131±131	- 4.5±2.9	65907	0.850	1.1	17545
686.1	8847	- 5.6±3.0	83918	0.846	1.1	17846

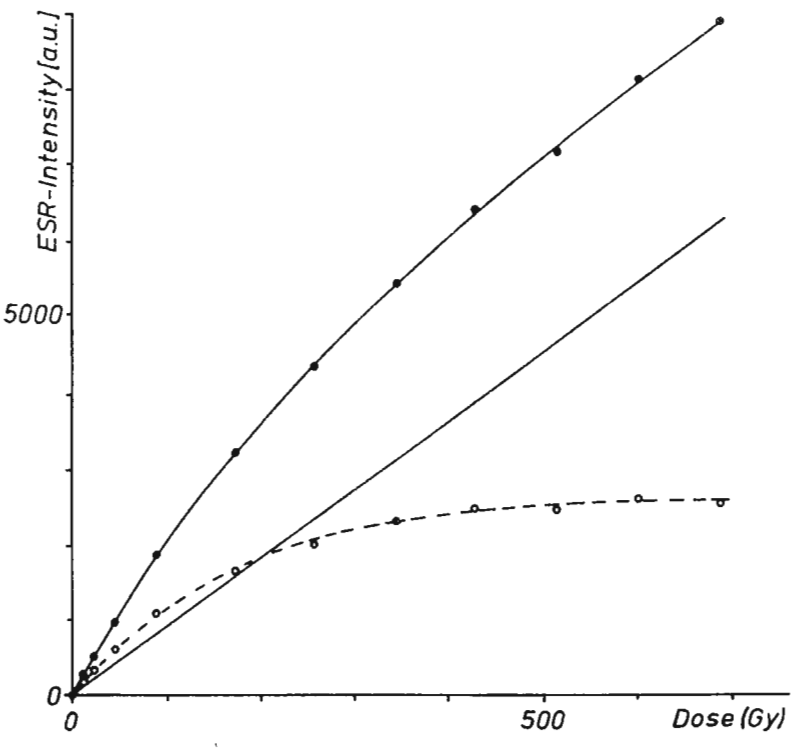

Figure 1.
Dose response of the paramagnetic centre at g = 2.0007 in corals. The closed circles show the averaged, normalized data set (see Table 2). The curve through these points is the sum of the lower two curves. The open circles result from the subtraction of the straight line from the original data set. The dotted line is the best exponential fit for the open circles.

Regression and error analysis for a saturating-exponential-plus-linear model

G. W. Berger
Department of Geology, Western Washington University, Bellingham, WA 98225, U.S.A.

Introduction

One tool helpful in attempts to attain accurate TL dates of both unheated sediments and heated material is the use of accurate extrapolation methods for laboratory TL dose-response curves. Berger and others (1987) have described a rapid and accurate (Berger and Huntley, 1989) regression and error analysis method for the simple saturating exponential model of dose response. However, with an increasing effort to date accurately geological material older than about 50 ka, I have frequently encountered dose-response curves that do not show saturation at high applied doses. The simplest model that adequately describes the data and which has a physical basis seems to be a saturating exponential with an added linear term.

As pointed out recently by Levy (1989, equation 4), linear TL buildup beyond an apparent saturation stage is just one of several forms of high-dose response curves that have been observed in the color center and radiation damage literature over the past two decades. Examples of geological quartz that exhibit either this added linear or a more general added supralinear response have been summarized by Fleming (1979), for example. An added linear response may manifest creation of defect traps simultaneous with trap filling during laboratory irradiation.

To allow more accurate extrapolation from one such "multi-stage" dose-response curve, I outline here modifications to the equations of Berger and others (1987) (hereafter denoted BLK87) that allow their regression and rapid error analysis procedure to be applied to the simple exponential-plus-linear model. The use of these modifications is illustrated with an application of the additive-dose method to fine-grained volcanic glass about 170 ka old. These modifications can also be applied straightforwardly to the partial-bleach method used for unheated sediments.

Regression

Using the terminology of BLK87, the modified fitting function is

$$f(D, \theta) = a(1 + \exp[-b(d+D)]) + mD \qquad (1)$$

where D is applied dose (in units of irradiation time to avoid inclusion of systematic error from dose calibration factors), θ is a vector of four regression parameters (or coefficients), and a, b, d and m are these coefficients.

As outlined by BLK87, the Gauss-Newton algorithm for linearizing equation (1) and the quasi-likelihood method (e.g., Dobson, 1990; Seber and Wild, 1989) of regression are used to obtain best estimates of the four coefficients. As before, $w_j = f^{-2}(D_j,\theta)$ is a weighting element (for the j^{th} data point) of the function (1) in the quantity R to be minimized.

The weighted-residual function $R(\theta)$ (BLK87 equation 7)

$$R(\theta) = \sum_{j=1}^{n} w_j \left[Y_j - f - \sum_{k=1}^{4} \beta_k G_k (D_j)\right]^2 \qquad (2)$$

is modified by extending the parameter summation k from 3 to 4 so that $G_4(D_j) = \partial f/\partial m = D_j$ from (1) above. Thus the j^{th} row in the design matrix X (BLK87 equation 9) becomes simply

$$[1 - e_j, a_r (d_r + D_j) e_j, a_r b_r e_j, D_j] \qquad (3)$$

where $e_j = \exp[-b_r (d_r + D_j)]$ and the subscript r denotes the r^{th} iteration of BLK87 equation 9. Equations 9 and 8 of BLK87 can then be used as outlined there to update the parameter estimates and iterate equation 9 until the required degree of precision is obtained.

In the case of the additive-dose method dealt with here, the required equivalent-dose value (D_e) is not equal to the coefficient d in equation (1) above (as it is in the simple saturating exponential model) but must be obtained by numerical solution of f = 0. For this the standard Newton-Raphson procedure is used.

Error analysis

The variance in this additive-dose D_e is calculated from equation 17 of BLK87, with terms for the second growth curve (required for the partial bleach method) being dropped so that

$$\Delta^2 = \frac{V^t \psi V}{|\partial f/\partial D|^2}$$

Here the extended variance-covariance matrix ψ is related to the information matrix I (BLK87 equations 14 and 10) for which the elements are calculated with BLK87 equation 11. For the model in (1) I becomes a symmetric 4 x 4 matrix with added elements I_{am}, I_{bm}, I_{dm}, I_{mm}, and their symmetric counterparts (e.g., $I_{ma} = I_{am}$). Note that for the saturating exponential, subscript c of BLK87 has been replaced by subscript d, as explained in BLK87. Because of the form of (1) above, the original nine elements of I (Appendix C of BLK87) do not change here.

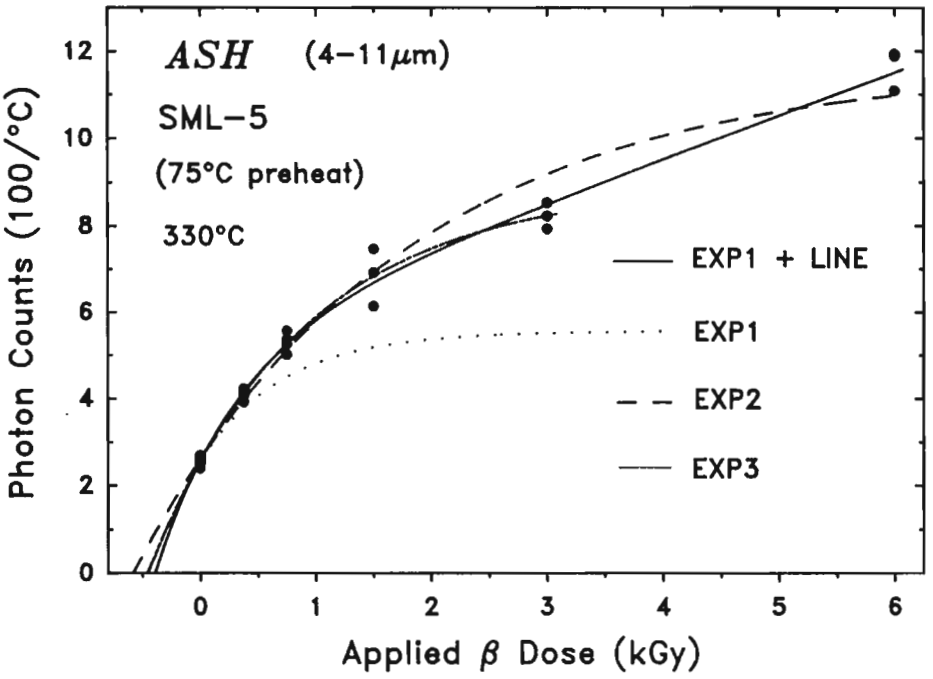

Figure 1.
Additive-dose data for purified volcanic glass from sample SML-5 at the 321-330 °C temperature zone of the glowcurves, preheated for 8 days to remove unstable TL. There are three weighted best-fit curves: EXP1+LINE (x-axis intercept 39151 Gy), EXP2 (intercept 582 ± 51 Gy), and EXP3 (intercept 456 ± 34 Gy). The intercept for the imbedded EXP1 curve is 443 Gy (error not computed).

Applying BLK87 equation 11 to (1) above we obtain for the additional matrix elements of I

$$I_{am} = a^{-1} \sum_{j=1}^{n} \frac{D_j}{f_j}, \qquad I_{bm} = \sum_{j=1}^{n} \frac{(d+D_j)D_j}{S_j f_j},$$

$$I_{dm} = \sum_{j=1}^{n} \frac{D_j}{S_j f_j} \quad \text{and} \quad I_{mm} = \sum_{j=1}^{n} \frac{D_j^2}{f_j^2}$$

where $S_j = \exp[b(d+D_j)] - 1$.

Similarly applying BLK87 equation 16 to (1) gives us the additional fourth element ($\partial f/\partial m$) of the transpose vector V^t, that is, D_e. The first three elements of V^t remain unchanged (Appendix D of BLK87). Finally, the partial derivative in the denominator of (4) above becomes abe + m, where $e = \exp[-b(d+D_e)]$.

Application

Data from the 321 - 330 °C glow-curve interval for a purified (by high-speed centrifugation using heavy liquids) volcanic ash sample of about 170 ka old are shown in Figure 1. The calculated D_e values define a plateau (over the interval 321 - 410 °C) only for the exponential-plus-linear fit in Figure 1. A plateau is not observed otherwise. Figure 1 also shows the poor fit of the saturating exponential model to the entire data set (EXP2), with a concomitant overestimate (582 ± 51 Gy at 330 °C) of the De value.

Discussion

The main motivation for using a large applied dose range in constructing dose-response curves is to minimize the range of extrapolation and therefore the error in the D_e value. However, for a fixed number of data points an increase in fitting parameters from 3 to 4 increases the error in the extrapolation. This effect is seen here in the somewhat larger error (± 51 Gy) for the preferred EXP1+LINE fit compared to the EXP3 fit (±34 Gy) in spite of the additional 3 data points (at 6 kGy). Nevertheless, had the new model been considered when these data were generated, then additional points in the 1.5 - 6 kGy range could have been produced to better constrain the linear term and thereby reduce the error in the D_e value. Thus for optimum use of the EXP1+LINE model, considerably more data may need to be generated than for the simple exponential model.

Alternatively, if the simple exponential model is applied to only a limited range of the applied dose values (e.g., EXP3 in Fig. 1) then unacceptably large extrapolations may be required for older samples than this example, and selection of these truncated data points may require unjustifiable subjectivity. Moreover, this use of truncated data may cause an artificial failure of the

plateau test, as observed with the sample in Figure 1. The plateau test failed probably because truncation at a constant dose value for all temperature points was inappropriate for this sample. Even if truncated regression does yield a plateau, the resultant TL age is merely "a model age".

Is the EXP+LINE regression model "physically realistic" ? I have several data sets (for both glass-rich ash and feldspar-rich sediments) for which this model clearly produces better fits than does the simple exponential model. One of these data sets (for a feldspar-rich sediment) appears to require an even more complicated EXP+SUPRALINEAR model. This observation is consistent with the general emphasis of Levy (1989) that a range of high- dose-response behaviour may be expected, and that the EXP+LINE model is just one of several physically realistic models. As stated by Levy (1989), equation (1) above may represent continual creation of defects throughout the burial history.

Data such as in Figure 1 also suggest the need for reconsideration of empirical comparisons of natural and laboratory "saturation" levels of TL in feldspars for the purpose of making corrections for long-term fading (e.g. Mejdahl, 1989; Hütt and Jaek, 1989). The usual assumption that the "efficiency" of defect creation is insignificant except at very high doses may need reassessment. Such defect creation can give the appearance (e.g., EXP3 in Figure 1) of a higher "saturation" level than is appropriate for simple trap filling alone.

Finally, several (but not all) of my data sets for old samples suggest that equation (1) is a more realistic approximation to the underlying (undetermined) physical processes than is the simple saturating exponential. In the author's general dating applications (wherein final accuracy is assessed by comparison with at least one independent control age for a sample suite) the stage has not yet been reached where routine application of yet more complicated models (e.g. the sum of equations 6 and 7 of Levy, 1989) is justifiable.

Acknowledgment

I thank R. A. Lockhart of the Department of Mathematics and Statistics, Simon Fraser University, Burnaby, B.C., for pointing out to me the nature of the modifications needed to accommodate the model dicussed here. I also thank the reviewer for helpful comments.

References

Berger, G. W., Lockhart, R. A. and Kuo, J. (1987) Regression and error analysis applied to the dose-response curves in thermoluminescence dating. *Nucl. Tracks & Radiat. Measts.*, **13**, 177-184.

Berger, G. W. and Huntley, D. J. (1989) Test data for exponential fits. *Ancient TL*, **7**, 43-46.

Dobson, A. J. (1990) An introduction to generalized linear models. Chapman and Hall.

Fleming, S. J. (1979) *Thermoluminescence techniques in archaeology*. Clarendon Press.

Hütt, G. and Jaek, J. (1989) The validity of the laboratory reconstruction of palaeodose. *Ancient TL*, **7**, 23-26.

Levy, P. W. (1989) Principles determining the length of time materials can be dated by TL, ESR and other trapped charge buildup methods. In *Occasional Publication no. 9*, The Research Laboratory for Archaeology and the History of Art, Oxford University, pp 24-29.

Mejdahl, V. (1989) How far back: life times estimated from studies of feldspars of infinite ages. op.cit., *Occasional Publication no. 9*, 43-48.

Seber, G. A. F. and Wild, C. J. (1989) *Nonlinear regression*. John Wiley and Sons.

PR D.J. Huntley

Internal dose rates of quartz grains separated from fault gouge

Rainer Grün[§] and Clark Fenton[†]
[§]Sub-department of Quaternary Research, Cambridge University, Free School Lane, Cambridge CB2 3RS, UK.
[†]Dept. of Geology & Applied Geology, University of Glasgow, Glasgow G12 8QQ, UK.

In TL/ESR investigations it is often assumed that quartz is basically free of radioactive elements and that therefore the internal dose rate is negligible. The few measurements that have been rarely carried out, yielded internal dose rates in the range of about 60 to 200 μGy/a (e.g. Sutton & Zimmerman 1978, Mejdahl 1987).

In course of an ESR dating study of quartz separated from fault gouge of various sites in Scotland, we have analyzed the U, Th, and K concentrations of the quartz separates as well as the bulk gouge sample by means of neutron activation analysis (NAA).

Samples of the soft clay-like fault gouge were wet sieved through a series of mesh sizes (500 - 63 μm). After storing in 10% HCl for 24h, the samples were washed in de-ionized water and etched with 35% fluorosilicic acid (H_2SiF_6) for 30h to remove feldspars. After washing, the residue was etched with 50% tetra-fluoboric acid (HBF_4) at 30 °C for 48h to remove mica (mica-rich samples were 'rolled' in a cellophane film to remove the bulk of such grains). After further washing and air drying the samples were passed through a Franz isodynamic separator at a current of 2 A to separate a dominantly quartz, non-magnetic fraction. If the remaining sample contained notable amounts of pyrite, they were given a 24h bath at 50 °C in conc. nitric acid (HNO_3). The remaining sample was then put in hydrofluoric acid (HF) for 2 h to remove a surface layer of about 20 μm that has been subject to external - radiation. A final washing in de-ionized water in a sonic bath for 30 min removed any traces of acid and any particles adhering to the surfaces of the grains. Any remaining non-quartz grains were removed by hand picking under a binocular microscope.

Table 1 gives the sample locations, grain sizes and a short macroscopic and microscopic description of the samples. The macroscopic colours are either associated with mica inclusions or the occurrence of coloured grains, which can be attributed to iron (orange - yellow), copper (green-blue), Fe_2O_3 and Al_2O_3 (purple), Al_2O_3 (dark brown) or Li_2O or MnO (red) in the crystal lattice. White frosty grains are due to a large amount of fluid inclusions in the crystals and HF attack on the grain surfaces. The 'aggregates' are quartz- muscovite intergrowths, a slight yellow coloration can be attributed to pinite. Some samples were X-rayed and the results are also described in table 1.

Table 2 gives the neutron activation results, beta self absorption factors (after Mejdahl 1979) and calculated dose rates using an assumed alpha ef- ficiency of 0.1 and dose rate conversion factors from Nambi & Aitken (1986). The detection limits of the analyses are 0.1 ppm for U and Th and 0.01% for K. The external beta and gamma dose rates are infinite matrix doses for the respective grain sizes calculated from the NAA results of the bulk gouge samples. The correct value may vary due to radioactive inhomogeneity at the site and variable water contents (mainly for external beta dose rate).

As can be seen from table 2, the concentration of radioactive elements in the quartz separates is rather small compared to that of the respective bulk samples. This leads also to relative small contribution of the internal dose rates to the total dose rate (0.4 to about 7%, in one case 18.9%).

It is remarkable that the separates with low concentrations of U and Th can already be macroscopically recognized. All white samples (except 714B and 717B) have U and Th concentrations below 0.5 ppm. Higher concentrations are connected with colour changes. In the coarser fractions, the internal dose rate of the essentially pure quartz separates does not exceed 3% of the total dose rate. In the finer fractions of these separates, the internal dose rate is lower than 4%. The internal beta dose rate rarely exceeds a third of the internal alpha dose rate and seems therefore negligible although K-concentrations of more than 1% have been measured. Mejdahl (1987) suggested a relationship between U and Th concentrations in quartz. The plot of U- concentration versus Th concentration (without samples 713A and 718B) yields a regression line with Th(ppm) = 1.53 U(ppm) - 0.111. The correlation coefficient is 0.812.

The XRD analysis was not particular conclusive. Sample 718B with the highest concentration of radioactive elements shows besides a quartz spectrum only one additional peak at 3.534 . Samples 723B and 725B show some peaks between 2.56 and 4.44, which could not clearly be attributed to common minerals. The other runs yielded basically pure quartz spectra.

In case of the more contaminated separates, the higher concentrations of radioactive elements seem to be linked to the occurrence of non-quartz minerals and hence, the calculated internal dose rate may be an overestimate. The conclusion of the present study is that the internal dose rate is indeed only a minor contribution to the total dose rate. However, the external dose rate is exceptionally high (4,000 to 19,000 μGy/a), the host rock consists of pegmatites or of Precambrian metamorphic rocks. In many environments such as beach sands or sand dunes, an alpha dose rate of about 120 %Gy/a as generated by

0.3 ppm U and 0.5 ppm Th does not seem to be negligible. In these cases it also does not seem advisable to calculate the Th concentration from the U- analysis, because this procedure may cause a large uncertainty in the assessment of the internal Th dose rate.

References

Mejdahl, V. (1979) Thermoluminescence dating: beta-dose attenuation in quartz grains. *Archaeometry*, **21**, 61-72.

Mejdahl, V. (1987) Internal radioactivity in quartz and feldspar grains. *Ancient TL*, **5**, 10-17.

Nambi, K. S. V. & Aitken, M. J. (1986) Annual dose conversion factors for TL and ESR dating. *Archaeometry*, **28**, 202-205.

Sutton, S. R. & Zimmerman, D. W. (1978) Thermoluminescence dating: radioactivity in quartz. *Archaeometry*, **20**, 67-69.

PR Vagn Mejdahl

Table 1. Description of the samples

No.	Site	Grain size (μm)	Colour	Comments
710	Glen Gloy (W)	250-355	grey	mica inclusions, few red grains; quartz: fractured with frosty surface XRD: nearly pure quartz
711A	Glen Gloy (E)	250-355	grey	as 710, fewer inclusions; quartz: fractured with frosted surface, some transparent not f ractured
B		125-180	grey	as 711A, some fine grained aggregates
712A	Kinloch Hourn	250-355	white	nearly pure quartz: extremely fractured, frosty surface, some clear transparent
B		125-180	brown	many yellow-red grains; quartz: mostly fractured with frosty surface, some clear transparent. XRD: pure quartz
713	Glen Elchaig	250-355	grey	few mica inclusions, many yellow or red fractured grains; quartz: slightly fractured frosty surface, more transparent clear grains
714A	Scardroy 1 (NE)	250-355	brown	Some red grains, mixture of fine grained aggregates and quartz: not strongly fractured, frosty surface. XRD: quartz, small mica peaks.
B		63-125	white	nearly pure quartz, most frosty surface, many transparent
715A	Scardroy 1 (SW)	180-250	brown-grey	some red-yellow grains, quartz: not strongly fractured, frosty surface
B		63-125	brown-grey	few yellow grains, quartz: most with frosty surface, some fine grained aggregates, some clear transparent. XRD: pure quartz
716A	Scardroy 2	250-355	brown-grey	some mica inclusions, rock fragments, quartz: half frosty, half clear transparent, some fine grained aggregates
B		63-125	grey	yellow red grains; quartz: mixture of frosty and clear transparent grains
717A	Scardroy 3	250-355	white	nearly pure quartz: not strongly fractured, most with frosty surface, some clear transparent
B		63-125	white	few yellow red grains, quartz: many fractured with frosty surface, some clear transparent
718A	Scardroy 4	250-355	grey-red	many yellow red grains, biotite/hornblende inclusions; quartz: fractured with frosty surface, few clear
B		63-125	grey-red	many red yellow grains, rock fragments, biotite/hornblende and pyrite inclusions; quartz: heavily fractured with frosty surface, few clear transparent. XRD: quartz, one unidentified peak
719A	Scardroy 5a	250-355	white	nearly pure quartz: some heavily fractured frosty, many non-fractured and clear transparent
B		63-125	white	nearly pure quartz: some heavily fractured, rest in every transition between frosty and clear transparent. XRD: pure quartz
720A	Scardroy 5b	180-250	grey-brown	few yellow red grains; quartz: not strongly fractured, most with frosty surface, some clear transparent surface, some fine grained aggregates
B		63-125	white	nearly pure quartz: some heavily fractured, rest in every transition between frosty and clear transparent
721A	Scardroy 5c	250-355	white	nearly pure quartz: fractured with frosty surface, few clear transparent
B		63-125	white	nearly pure quartz: some heavily fractured, rest in every transition between frosty and clear transparent
722A	Scardroy 5d	250-355	white	nearly pure quartz: mixture of fractured frosty and clear non fractured grains
B		63-125	white	nearly pure quartz: some heavily fractured, rest in every transition between frosty and clear transparent
723A	Invershiel	250-355	white	nearly pure quartz: mixture of fractured frosty and clear non-fractured grains
B		63-125	brown	many yellow red grains; quartz: mostly clear transparent, rest partly fractured with frosty surface. XRD: quartz, some other non-determined peaks
725A	Coire Eoghainn (Glen Cannich)	250-355	grey brown	many red yellow grains and fine grained aggregates; quartz: fractured with frosty surface, few clear. XRD: pure quartz
B		63-125	brown	many yellow red grains and fine grained aggregates; ferric inclusions; quartz: dominantly with frosty surface, many clear transparent XRD: quartz, some other determined peaks

Table 2: Analytical results and dose rate calculations

Sample No.	U (ppm)	Th (ppm)	K (%)	absorbed fraction of ß dose rate U	Th	K	internal dose rate ß (µGy/a)	α	external dose rate ß (µGy/a)	internal dose rate (%)
710Bulk	36.4	30.0	6.4						7255	
A	0.6	1.0	0.84	0.19	0.25	0.11	99.2	240.8	9625	2.0
711Bulk	12.5	21.0	3.8						3439	
A	0.5	0.7	0.26	0.19	0.25	0.11	42.3	190.8	4699	2.8
B	1.3	2.0	0.99	0.12	0.18	0.05	73.7	509.3	5056	6.4
712Bulk	10.7	18.0	5.5						3491	
A	0.3	0.3	0.02	0.19	0.25	0.11	12.3	105.6	5651	1.3
B	0.9	1.6	0.27	0.12	0.18	0.05	35.2	368.5	6067	4.1
713Bulk	9.9	29.0	4.6						3755	
A	0.6	3.2	0.35	0.19	0.25	0.11	71.3	403.3	5143	5.1
714Bulk	4.7	27.0	5.0						3157	
A	1.0	2.5	0.64	0.19	0.25	0.11	103.4	462.8	4771	6.7
B	1.0	0.4	0.01	0.09	0.14	0.03	15.1	307.7	5251	3.7
715Bulk	2.7	4.2	5.1						1766	
A	0.5	0.6	0.15	0.15	0.21	0.08	24.4	183.4	4254	3.3
B	1.0	1.1	0.22	0.09	0.14	0.03	23.1	359.4	4494	5.8
716Bulk	1.5	9.0	4.2						1661	
A	0.3	0.5	0.17	0.19	0.25	0.11	27.2	120.4	3418	2.8
B	0.6	0.6	0.07	0.09	0.14	0.03	12.1	211.2	3743	4.0
717Bulk	1.0	7.4	4.5						1594	
A	0.3	0.1	0.07	0.19	0.25	0.11	15.3	90.8	3541	2.0
B	1.0	0.4	0.12	0.09	0.14	0.03	17.8	307.7	3873	5.6
718Bulk	3.3	21.0	4.0						2442	
A	1.2	1.0	0.04	0.19	0.25	0.11	44.3	407.6	3749	6.8
B	4.2	3.8	0.32	0.09	0.14	0.03	78.8	1448.8	4125	18.9
719Bulk	1.7	12.0	5.2						2083	
A	0.1	<0.1	0.01	0.19	0.25	0.11	3.7	27.8	4232	0.5
B	0.4	0.2	0.01	0.09	0.14	0.03	6.3	126.0	4634	1.9
720Bulk	3.6	9.9	5.3						2214	
A	0.3	0.5	0.20	0.15	0.21	0.08	22.7	120.4	4647	2.0
B	0.3	0.3	0.01	0.09	0.14	0.03	5.4	105.6	4915	1.5
721Bulk	1.7	8.6	5.2						1906	
A	0.1	<0.1	0.02	0.19	0.25	0.11	4.6	27.8	4158	0.5
B	0.3	0.2	0.02	0.09	0.14	0.03	5.3	98.2	4549	1.6
722Bulk	1.3	9.2	3.2						1406	
A	0.1	0.1	0.03	0.19	0.25	0.11	6.2	35.2	2674	1.0
B	0.4	0.3	0.04	0.09	0.14	0.03	7.5	133.4	2931	3.1
723Bulk	34.5	42.0	7.0						7811	
A	0.1	0.4	0.09	0.19	0.25	0.11	13.8	57.4	10094	0.4
B	1.6	3.1	1.00	0.09	0.14	0.03	58.1	674.1	11192	3.7
725Bulk	5.2	28.0	5.2						3315	
A	0.4	1.1	0.17	0.19	0.25	0.11	34.4	192.5	4997	2.7
B	1.2	2.1	1.60	0.09	0.14	0.03	63.5	488.9	5501	5.9

Isolation of the rapidly bleaching peak in quartz TL glow curves

A. D. Franklin and W. F. Hornyak
Physics Department, University of Maryland, College Park, Maryland 20742, USA.

Introduction

Natural archaeological and geological quartz, without additional laboratory doses, often exhibits two major TL peaks: a rapidly bleaching peak (RBP) at about 325 °C, for a ramp rate of 20 °C/s. (Fleming, 1979; Spooner et al, 1988). In the work reported here the ramp rate was considerably lower at 1°C/s. This difference in ramp rate is accompanied by a downward shift in TL peak temperatures, so that in our data the RBP occurs at about 275 °C and the SBP at 310-330 °C, depending on the optical filter used. Expected plateau ranges are likewise shifted downward. The RBP is currently the basis for work on optically stimulated luminescence dating (Huntley et al., 1985; Smith et al., 1986; Godfrey-Smith et al., 1988; Rhodes, 1988).

To make possible direct study of the RBP we have devised a method of isolating this peak by combining use of optical filters during measurement with a subtraction technique, in which a TL glow curve taken after apparently complete removal of RBP by optical bleaching is subtracted from the corresponding glow curve obtained before bleaching to yield the RBP by difference.

To obtain a pure quartz, sand was extracted from samples drawn from the relic dunes at Dobe - toa in the northwest Kalahari desert of southern Africa (Helgren and Brooks, 1983; Helgren, 1982), part of a site of considerable archaeological interest. The sediment was treated at room temperature with 3N HCl to remove carbonates, 48% HF followed by 3N HCl to remove alkali feldspars and fluorides, and H_2O_2 to remove organics. The 90-150 μm fractions was selected by sieving, and then density separated to isolate the quartz component with density <2.70 g/cm^3. The resulting freely-flowing powder was light buff in color and was composed of rounded transparent grains, most of which were shiny and clear. The x-ray powder diffraction revealed only excellent α-quartz patterns.

The RBP has in the past for the most part been observed using broad banded blue (e.g. Corning 5-60) or violet (e.g. Corning 7-59) optical filters in conjunction with a PM tube such as the EMI 9635Q. In order to separate the RBP and SBP as much as possible we have examined the spectral output of our quartz after laboratory irradiation, across the near u.v. and visible regions. In keeping with data in the literature (Schlesinger, 1964; Medlin, 1968; Zimmerman, 1971; Fuller and Levy, 1977, 1978; David et. al., 1977) we find emission peaks centered around 490 nm with glow peaks at 190 and 330 °C and perhaps at higher temperatures, using a ramp rate of 1°C/s. In the wavelength region below about 400 nm major glow peaks occur at 70, 180, 275 and 310 °C, and minor peaks are seen at ~125 and ~240 °C.

The peak at 275 °C, strongly emitting below 400 nm, is the RBP. It cannot be completely isolated by the use of filters but it can be maximized relative to the SBP by using a uv filter such as the UG11. Spooner et. al. (1988) showed that RBP can be rapidly and completely bleached with long wavelength (e.g. green ~2.3 eV) light with essentially no effect on the SBP. Thus (fig. 1) the RBP can be obtained by subtraction of the glow curve after the green-light bleach from the glow curve with no bleach.

A subtraction technique demands the utmost in precision, with respect to both TL intensity and temperature. Weight-normalized glow curves obtained with the sample essentially as described earlier (Franklin et al., 1987) are averaged over up to 16 runs. A temperature marker is placed on each by exposing the sample to a very small standardized beta-dose, the ZG dose, using a Sr-90 source prior to the run but after a brief (three minute total, including 1 °C/s rise time) preheat to and hold at 150 °C. The purpose of the preheat is to remove low-temperature TL induced in artificially irradiated samples. The ZG dose generates an easily measurable peak at 70 °C which is used to normalize temperatures.

The resulting averaged glow curves still contain uncertainty in TL intensity and in temperature. The uncertainty in TL of the unbleached curve relative to the bleached curve can be reduced by normalizing the former to the latter using the ratio of intensities of the average 70 °C peaks. Some further adjustment along the temperature axis is necessary because the use of the Au/Ni plate Cu bowl as a specimen holder introduces a small variable effect on the rate of the rise of the temperature of the sample. This adjustment was made in present data by maximizing the coincidence of the unbleached and bleached glow curves on the high temperature side of the SBP. The results of these procedures are data such as illustrated in figure 1 for laboratory-irradiated samples.

First Glow Growth Curve

RBP glow curves for laboratory doses from 0 to 300 Gy added to the natural dose are shown in figure 2. Experimental standard deviations for the TL value range from 6% to 13%. The curve for 300 Gy is apparently saturated, higher laboratory doses up to 1 kGy yielding essentially the same curve. The first glow growth curve for the temperature at the glow curve peak (275 °C) is shown in figure 3a. Because if the apparent sudden

onset of saturation at 300 Gy no attempt has been made to fit with a saturating exponential equation. These data can be used to obtain an estimate of the intercept on the dose axis. A simple unweighted linear squares fit to the first four data points produced a value for the intercept of 40 Gy. The lσ confidence interval (treating the four fitted data points in figure 3a as single values) is shown as a small heavy line on the abscissa at the intercept. The intercepts, from several such glow growth curves, produce a reasonable plateau from 240 to 290 °C, shown in figure 3b. This figure suggests a mean intercept of 42 ± 1 Gy.

Conclusion

By use of an ultraviolet band pass filter, careful TL measurements, and appropriate data manipulation, the rapidly bleaching TL peak in quartz for doses in the range 0 - ~200 Gy can be isolated and studied independently of the nearby slowly bleaching peak. For a sample of the average radioactivity discussed by Aitken (1985, p. 68), this suggests and upper limit to the age determination of about 70 ka. However many samples exhibit much less radioactivity and the age limit could be much higher, limited eventually by the lifetime of the RBP, estimated at ~10^8 years (Aitken, 1985, p. 272).

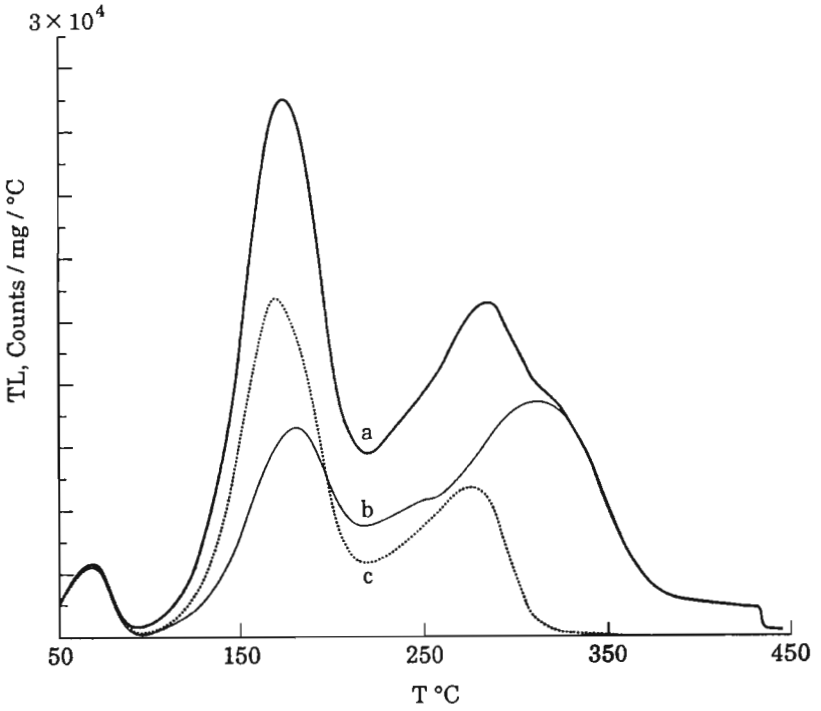

Figure 1.
TL glow curves for Kalahari dune sediment, 90-150 μm quartz fraction given 100 Gy Co-60 gamma dose: a) without light exposure; b) with 4 hour exposure to solar simulator with Chance-Pilkington 26-3350 green filter; c) difference curve.

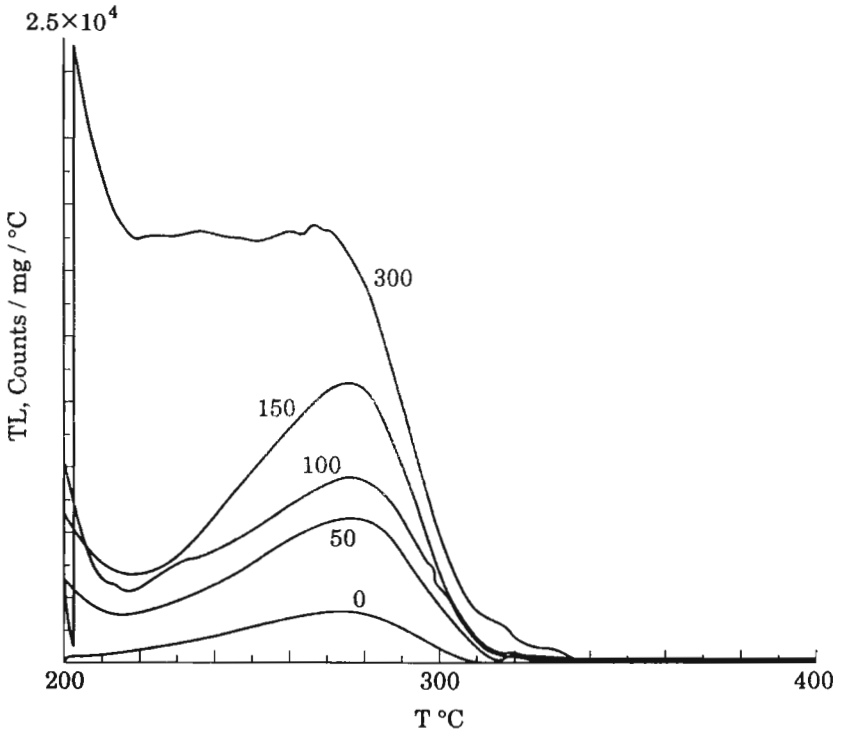

Figure 2.
Rapidly Bleaching Peak (RBP) TL glow curves for 90 - 150 μm quartz fraction of Kalahari dune sediment given Co-60 gamma doses shown (in Gy).

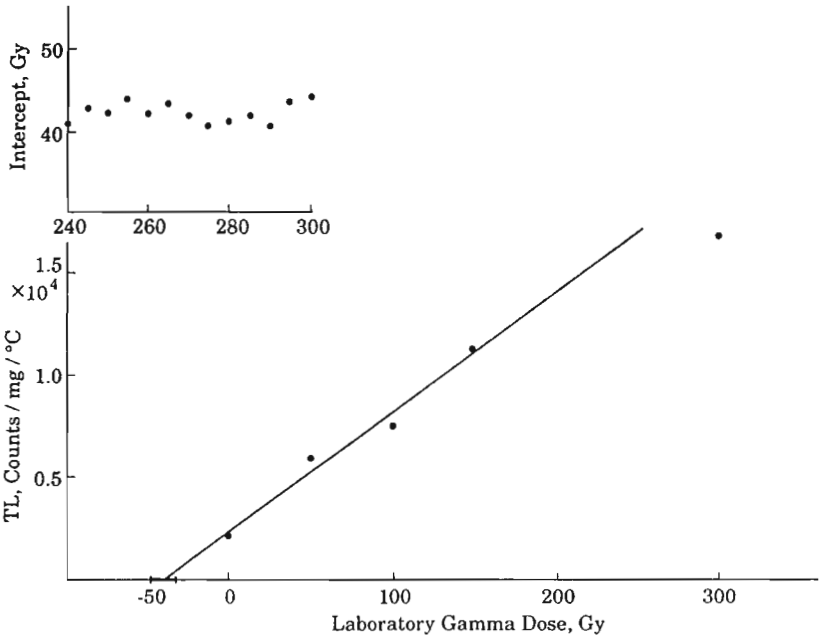

Figure 3.
First flow growth data from Rapidly Bleaching Peak (RBP) for 90 - 150 μm quartz fraction of Kalahari dune sediment: a) first glow growth curve using glow curve peak values (275 °C). Heavy line at intercept represents 1σ confidence interval; b) intercept at several temperatures.

Acknowledgements
This work was supported by the National Science Foundation under grant number BYS-8911758. The authors are grateful to Anne Tschirgi, James Broomsfield, and William Dickerson for TL measurements and other help.

References

Aitken, M. J. (1985) *Thermoluminescence dating*, Academic Press, London.

David, M., Sunta, C.M., and Ganguly, K. (1977) Thermoluminescence of quartz: Partl - glow curve and spectral characteristics, *Ind. J. Pure and Appl. Phys.*, **15**, 201-4.

Fleming, S.J. (1979) *Thermoluminescence techniques in archaeology*. Clarendon Press, p46.

Franklin, A.D., Hornyak, W.F., and Tschirgi, A. (1987) Experimental TL Techniques for the inclusion method, *Ancient TL.*, **5**, 9-10.

Fuller, E.G. and Levy, P. (1978) Thermoluminescence of natural quartz, *Bull. Am. Phys. Soc.*, **23**, 324.

Godfrey-Smith, D.I., Huntley, D.J., and Chen, W.H. (1988), Optical dating studies of quartz and feldspar sediment extracts, *Quaternary Science Reviews*, **7**, 373-380.

Helgren, D.M. (1982) Edaphic context of the mongongo *(Ricinodendron rautanenii)* in the Northwestern Kalahari. *South African J. of Science*, **78**, 131-2.

Helgren, D.M., and Brooks, A.S. (1983) Geoarchaeology at Gi, a middle stone age and later stone age site in the Northwest Kalahari. *J. Archaeological Sciences*, **10**m, 181-197.

Huntley, D.J., Godfrey-Smith, D.E., and Thewalt, M.L.W. (1985) Optical Dating of Sediments, *Nature*, **313**, 105-7.

Medlin, W.L. (1968) Thermoluminescence in Aluminium-containing Quartz. *Physics Letters*, **10**, 49-50.

Rhodes, E.J., (1988), Methodological Considerations in the optical dating of quartz. *Quaternary Science Reviews*, **7**, 395-400.

Schlesinger, M. (1964) Thermoluminescence in quartz. *J. Chem. Phys.*, **38** , 1132-43.

Smith, B.W., Aitken, M.J., Rhodes, E.J., Robinson, P.D., and Geldard, D.M. (1986) Optical dating: Methodological aspects. *Radiation Protection Dosimetry*, **17**, 229-33.

Spooner, N.A., Prescott, J.R. and Hutton, J.T. (1988) The effect of illumination wavelength on the bleaching of the thermoluminescence (TL) of quartz. *Quaternary Science Reviews*, **7**, 325-9.

Zimmerman, J. (1971) The radiation-induced, increase of the 100 °C thermoluminescence sensitivity of fired quartz. *J. Phys. C. Solid State Physics*, **4**, 3265-76.

PR Helen Rendell

Dating quartz sediments using the 325 °C TL peak: new spectral data

John R. Prescott and P. J. Fox
Department of Physics and Mathematical Physics, University of Adelaide, Adelaide, Australia 5001.

Shortly after Mike Smith (1987) described the Puritjarra rock shelter in Australia's Northern Territory, the Adelaide Archaeometry group began collaboration with him to find thermoluminescence (TL) dates for the project one of the objectives being to check radiocarbon and thermoluminescence dates one against the other. The oldest C-14 age is 22,440 ±370 years. Samples (PJ1ES series) were taken within the shelter to a depth of 2.1 m which is much deeper than the apparent occupation, and from the dune field nearby (PJ2S series). We have since obtained a sequence of quartz inclusion TL dates from the site.

The TL ages provide consistent seriation with depth within the shelter. Ages agree well (3 ka) for test site PJ3S which was specially selected from the rear of the shelter with less likelihood of disturbance than for other sites. Most other comparisons suggest that the TL age is older than the most nearly corresponding C-14 age by five or six thousand years. This is a serious matter because it could be said to leave unresolved the true age of Puritjarra. However, the possibility of an error in TL methodology is even more serious for it would tend to bring into question TL dates in general.

Our feeling was that incomplete bleaching was the most likely cause for the discrepancy but we carried out extensive independent checks on other possibilities. These included repeat TL resampling of charcoal PL measurements on two samples and independent analysis for U, Th and K. We conclude that bleaching was incomplete for some samples although sampling problems for C-14 still remain possible.

We have carried out bleaching tests on a subset of the original samples as collected. They therefore included clay as well as quartz and it is i n this form that the original material would have been exposed to light. Samples PJ1ES/10 and PJ1ES/75 were exposed in thin layers to Adelaide summer sunlight and were found not to be well even after 21 days of summer sunlight. The PJ2S and PJ3S samples bleached rapidly to low levels and the surface samples from these two sites were found to have been already bleached, indicating long exposure to light in conditions presumed to reproduce the original conditions. This is consistent with the agreement between TL and C-14 ages for PJ3S and geomorphological arguments for the samples PJ2S from outside the shelter. Figure shows bleaching of glow curves for PJ1ES/75 with time as a parameter; it also shows the level to which bleaching proceeds in extracted and etched quartz samples.

It appears that resetting has been only partial a Puritjarra because the quartz used in the dating measurements is "shielded" from exposure to the sun by a thin layer of clay and/or iron oxide on the grains and because the orientation of the shelter virtually excludes direct sunlight.

The key question in dating bleached sediments is whether the materials (e.g quartz) have been exposed to sunlight for "long enough" to reset the TL clock. There are two schools of thought the "total bleach" and the "partial bleach" schools.

The total bleach school (e.g Singhvi et al, 1982) have argued that in the majority of cases the physical environment is such that essentially complete bleaching can be assured, although there is an inevitable element of judgement in this. The Adelaide group has tended to follow this philosophy (e.g Lu et al, 1988) and it was the philosophy used at Puritjarra in the first instance, because the materials were assessed as wind-blown sediments from an open site with long exposure. This turned out not to be true for all samples.

The partial bleach school, largely developed by Wintle and Huntley (1980) argue that since you do not know how much the sample has been bleached, then you should assume the worst and base your dating on a component in the TL that bleaches easily assuming that there is one. It has long been clear that there is such a component in quartz and Spooner et al (1988) confirmed that it is the 325 °C peak.

We have therefore devised a set of procedures which when used provide greater confidence in the degree of resetting. It is very similar to the procedure proposed by Franklin and Hornyak (1990).

Spooner et al (1988) showed that the 325 °C peak in the TL glow curve of quartz is extremely susceptible to bleaching by light of all wavelengths and that this continues to be true even in unseparated field samples; and we have confirmed this for PJ samples specifically. The half-intensity bleaching time by full sun is about twenty seconds for this peak and a few minute of full sun is sufficient completely to remove it. It can therefore be assumed that the conditions for "total bleach" were satisfied for this peak at the time of deposition and that TL ages determined from this peak by total bleach methods will be correct.

Fox (1990) has shown that the peak characteristically emits light peaked at 380 nm and that these wavelengths are selectively bleached. The 325 °C peak can therefore be selectively used for dating using suitable optical filters. Contour plots of the spectral data for a PJ1ES sample, glowed out and re-irradiated with 9 Gy before and after bleaching are reproduced in figure 2. In the unbleached sample, the 380 nm

emission ridges outwards from more intense emission peaking at 480 nm; after 40 s bleaching with 350 nm light it has gone.

The detector of the spectrometer is similar to that used for TL measurements and since the optical response of the spectrometer (without detector) is essentially wavelength independent, these spectral data are reproduced in their uncorrected form to illustrate the relative changes in spectral components of the TL emission which would be detected using a 9635Q PMT (with HA3). The spectrally-corrected response peaks in the red near 630 nm (inset fig. 2a). The easily-bleached "325 °C" peak appears at a temperature of 305 °C with the heating rate of 5 K/s used here. Apart from pre-dosing of the 110 °C peak, there was little change of the spectrum on reheating.

A suitable filter combination for isolating this peak with a 9635Q PMT is a UG-11 plus 7-59 (fig 3) which accepts 320-380nm and largely rejects other wavelengths that do not readily bleach. The UG-11 filter is a compromise between selection of the 325 °C peak and rejection of the neighbouring peaks; it does not fully isolate the former and the glow curve still has some contributions from other temperatures. The data in figure 1 were taken with the 7-59 filter; the inset in fig. 1 shows the enhanced response at 325 °C for the 7-59 + UG-11 combination. A UG-11 filter alone or a UG-2 filter is almost as satisfactory although the latter also transmits in the red.

Further, if as part of the laboratory dating procedures, bleaching is carried out only with light of wavelength longer than about 475 nm (eg using a GG-475 filter) it is possible selectively to remove the 325 °C peak without affecting any of the rest of the TL which can therefore be used as a baseline from which the 325 °C peak rise, and from which the 325 °C peak intensity can be found by subtraction as described by Franklin and Hornyak.

Application of these procedures to an artificially-aged sample recovered the correct dose and produced a reduction of the apparent age of PJ1ES/75 from about 30 ka to 22 ka. We are currently repeating the dating of PJ using the new techniques. We agree with Franklin and Hornyak that the amount of work involved is considerably more than is required for conventional total bleach dating. However this is a small penalty to pay to obtain more accurate dates.

Acknowledgements

This work was supported by the Research Committee of the University of Adelaide. Linh Nguyen assisted with many of the bleaching measurements. We thank Franklin and Hornyak for sending us a copy of their paper in advance of publication. The final version of this present paper was written with theirs in mind.

References

Fox, P. J. (1990) Optical studies of thermoluminescent materials. PhD thesis, University of Adelaide (unpublished).

Franklin, A. D., and Hornyak, W. F. (1990) Isolation of the rapidly bleaching peak in quartz TL glow curves. *Ancient TL*, this issue.

Lu Yanchou, Prescott, J. R and Hutton, J. T. (1988) Sunlight bleaching of the thermoluminescence of Chinese loess. *Quater. Sci. Rev.*, **7**, 335-338.

Singhvi, A.K., Sharma, Y. P. and Agrawal, D. P (1982) Thermoluminescence dating of sand dunes in Rajasthan, India. *Nature*, **295**, 313-315.

Smith, M. A. (1987) Pleistocene occupation in arid Central Australia, *Nature*, **328**, 710-711.

Spooner, N. A., Prescott, J. R and Hutton, J. T (1988) The effect of illumination wavelength on the bleaching of thermoluminescence (TL) of quartz. *Quater. Sci. Rev.*, **7**, 325-329.

Wintle, A. G and Huntley, D. J (1980) Thermoluminescence dating of ocean sediments. *Can. J. Earth Sci.*, **17**, 348-360.

PR Helen Rendell

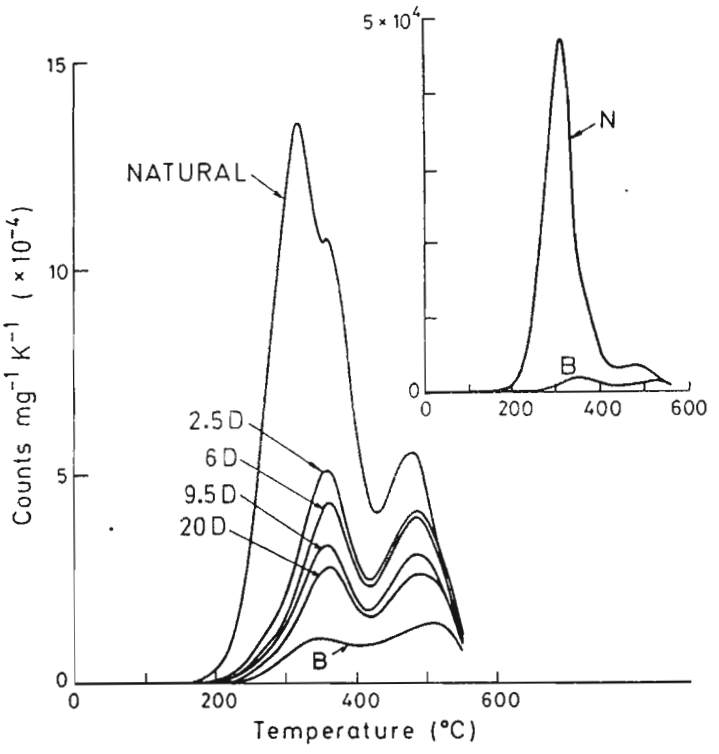

Figure 1
Glow curves for "natural" sample PJ1ES/75 before and after bleaching. Bleaching time are days of natural sunlight. Curve B is for extracted and etched quartz bleached for two days. The curves were obtained with 7-59 optical filter. For comparison purposes, the inset shows two corresponding curves using the filter combination 7-59 + UG-11.

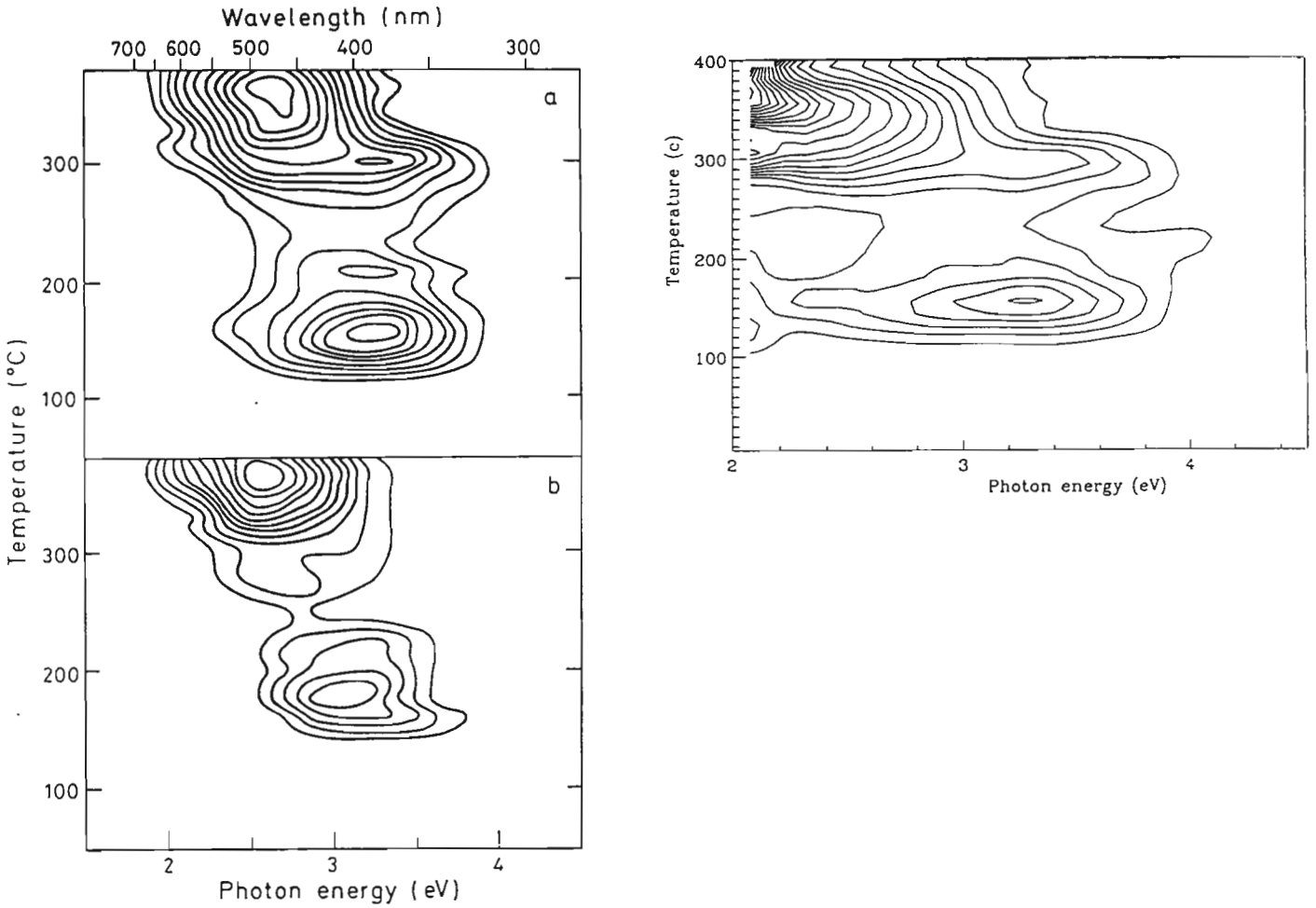

Figure 2.
Contour plots of the spectral data for a laboratory-irradiated PJ1ES sample.
(a) before bleaching (b) after 40s bleaching at 350 nm (2 mJ.cm^{-2}).
The wavelength scale is added for comparison purposes. The spectral intensities per unit bandwidth and kelvin are computed in energy space. The contour plot on the RHS is fig. 2a) corrected for instrument response.

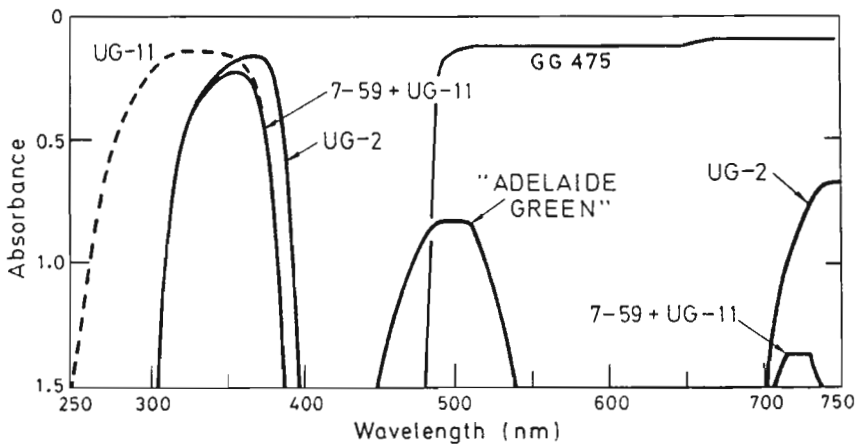

Figure 3.
Absorbance vs wavelength for some of the filters referred to in the text.

Comment

on *Regression analysis of exponential palaeodose growth curves*
by V. Poljakov and G. Hütt

G. W. Berger
Department of Geology, Western Washington University, Bellingham, WA 98225, USA.

Paljakov and Hutt (1990), hereafter denoted PH90, outlined a standard approach (see texts on nonlinear regression, e.g. Seber and Wild (1989) and references therein) to regression and error analysis for a saturating exponential model but failed to state why this simple approach differs from that proposed by Berger et al. (1987), hereafter denoted BLK87, for the additive dose method. Here I wish to clarify this omission.

Though the form (parameterization) of the exponential equation used in PH90 differs from that used by BLK87 (PH90 do not state why their equation is "more convenient"), this difference is not important here. What is distinct is the inclusion of a weighted error term in the functional expression of the model of BLK87. For this reason the implication by PH90 that their "straight minimization" method lacks certain disadvantages of the linearization method used by BLK87 is misleading. The simple minimization method of Ph90 is not applicable to the more complicated model of BLK87.

Though BLK87 believe that their regression and error model was the most realistic statistically (see their extensive discussion), subsequent comparisons of different procedures applied to sets of "good" data (Berger and Huntley, 1989) suggest that in many luminescence and ESR applications there may be no significant difference among the alternative procedures.

References

Berger, G. W. and Huntley, D. J. (1989 Test data for exponential fits. *Ancient TL*, **7**, 43-46.

Berger, G. W., Lockhart, R. L., and Kuo, I. (1987) Regression and error analysis applied to the dose-response curves in thermoluminescence dating. *Nucl. Tracks and Radn. Measts.*, **13**, 177-184.

Poljakovk, V. and Hutt, G. (1990) Regression analysis of exponential palaeodose growth curves. *Ancient TL*, **8**, 1-2.

Seber, G. A. F. and Wild, X. J. (1989) *Nonlinear regression*. John Wiley and Sons, New York, 743p.

Bibliography

Berger, G. W. (1990) Effectiveness of natural zeroing of the thermoluminescence in sediments. Journal of Geophysical Research, **95(B8)**, 12.375-12.397.

Cini Castagnoli, G., Bonino, G., Provenzale, A. and Serio, M. (1990) On the presence of regular periodicities in the thermoluminescence profile of a recent sea sediment core. Philosophical Transactions of the Royal Society, London, **A**, **330**, 481-486.

Galloway, R B (1990) Uranium and thorium series determination in natural samples by a beta-alpha coincidence technique. *Measurement Science Technology*, **1**, 725-730.

Liritzis, Ya (1989) Dating of Quaternary sediments by beta thermoluminescence: investigations of a new method. *Annales de la Societe Geologique de Belgique*, **112**, 197-206.

Proszynska-Bordas, H., Proszynski, M. and Stanska-Proszynska, W. (1989) Thermoluminescence chronology of fossil soils from profile of loessy and alluvial sediments in Samborzec-Polanow compared with TL datings of Eemian lacustrine and bog sediments. (in Polish) *Zeszyty Naukowe Politechniki Slaskiej*, **61**, 251-264.

Tejan-Kella, M. S., Chittleborough, D. J., Fitzpatrick, R. W., Thompson, C. H., Prescott, J. R. and Hutton, J. T. (1990) Thermoluminescence dating of coastal sand dunes at Cooloola and North Stradbrooke Island, Australia. *Australian Journal of Soil Research*, **28**, 465-481.

Wagner, G and Zoller, L. (1989) New methods of dating in geoscience research with particular reference to thermoluminescence. *Geographische Rundschau*, **41**, 507-512.

ESR or TL dates given in

Forman, S. L. and Maat, P. (1990) Stratigraphic evidence for late Quaternary dune activity near Hudson on the Piedmont of northern Colorado. *Geology*, **18**, 745-748.

Goede, A., Veeh, H. H. and Ayliffe, L. K. (1990) Late Quaternary palaeotemperature records for two Tasmanian spelethems. *Australian Journal of Earth Sciences*, **37**, 267-278.

Compiled by Ann Wintle.

Book details received:

Coyne, L.M. McKeever, S.W.S. and Blake, D.F. (1989) *Spectroscopic characterization of minerals and their surfaces*. ACS Symposium Series No 145. ISBN 0-8412-1716-5. LC 89-27755.

Computer Column

D. J. Huntley

The 'Nucleus' has announced a new plug-in multichannel scaling board for the PC. It is called the MCS-II and the price is US$ 995 in the USA. It will count at 200 MHz if the negative NIM input is used, or at about 50 MHz for TTL input. The board is a much cheaper alternative to the PCA board that I reviewed earlier (*Ancient TL*, 1988, **6(2)**, p18) because it does not perform pulse height analysis in addition to multi-channel scaling. It appears superior to the Ortec ACE MCS board in several respects. Of critical interest is the ease with which it may be operated with a program written by the user. The announcement indicates that it has the same software as the PCA board, and thus there should be little difficulty for those already using this board. Others are advised to consult the review of the PCA board and note that my program (written in Microsoft QuickBasic) for running the PCA is available.

Notices

First Notice

LUMDETR - 91

International Symposium
on
Luminescent Detectors and Transformers of Ionizing Radiation

October 9 - 11, 1991, Riga, Latvia

Scope

Fundamental problems of radioluminescence, photo- and thermo-stimulated processes in solids.

Physics and chemistry of luminophors for detection and transfer of ionizing radiation.

Luminescent image transformers for roentgenology, radionuclear diagnostic and defectoscopy.

Luminescent detectors for computer tomography.

Scintilators.

Luminescent detectors for dosimetry of ionizing radiation.

Application of luminescent detectors, transformers and dosemeters.

Language:
The official language of the symposium will be English.

Registration fee:
The registration fee is 200 US$ for participants and 65 US$ for acompanying persons.

Scientific programme:
The Symposium will include invited talks of 20-40 minutes and poster presentations. Separate discussions concerning problems of the scope of the Conference will be organized.

In order to obtain a Registration Form please contact Dr Ivars A. Tale at the address given below a soon as possible.

Deadlines for LUMDETR-91:

December 15, 1990 - return of registration form
February 15, 1991 - distribution of second circular
April 15, 1991 - deadline for abstracts of papers
June 1, 1991 - distribution of preliminary symposium program

Organizing commitee contact:
Dr Ivars A. Tale
Institute of Solid State Physics, University of Latvia
8 Kengaraga Str., 226063 Riga, Latvia
Phone O13-2-260-639, 013-2-262933 (secretariat)
Telex TEMA 161172 SU
Fax 013-2-225039

First Notice

2nd Southern-European Conference on Archaeometry

April 19-21, 1991, Athens, Greece

Theme

Science and the determination of early trade and contact of inter-mediterranean crossings, 7 th - 1st millennium B.C.

Topics
Dating methods
Provenance Studies
Analytical methods
Prospection
Computer approaches
Archaeoastronomy

***The deadline** for completed registration forms, obtained from the address given below, and abstracts is:*

January 15th 1991.

For further details please contact:

Dr Y Liritzis
Karneadou 13
106 75 Athens
Greece

tel: (01) 7230 913-15 fax: (01) 7230 676
telex: 214 386 EPKD

•Errata

Ancient TL 8(ii): *Moisture correction for annual gamnma dose* by M.J. Aitken and J. Xie.

The following paragraph from the Reviewer's Comments (John Prescott) for the above paper was unfortunately omitted:

> For Photons, readers may wish to note the more recent compilation of J.H. Hubbell (1982) Int. J. Appl. Radiat. Isotopes, 33, 1269-1290. and the discussion by R.K. Hobbie (1987) in Williams L.E. (Ed) *Nuclear Medical Physiscs*, Boca Raton, CRC Press. *Stopping powers for electrons and positrons* (1984) is another recent compilation.

•Electronic Mail

Electronic mail intended for *Ancient TL* should be sent to: Ian.Bailiff@uk.ac.durham - once you have gained access to the JANET network within the UK.

Ancient TL SUPPLEMENT

Date List

November 1990 Issue 4

1. This list includes dates for fired materials of archaeological interest, submitted to *Ancient TL* during 1989 for which sufficient information has been supplied. Readers are referred to earlier issues of the Date List for a fuller description of the structure of entries.

2. Application forms are available from the Editor, who will be pleased to advise on data compilation; laboratories wishing to submit dates for which the current date entry specification is not suitable should write to him. The application forms may be supplied on either paper or magnetic media.

Laboratory: [*name*] **Date Entry Specification** **Entry:** [*entry number*]

PART I

Site: [*Name*] **Location:** [*Region, country*] **Grid Ref.:** [*National map reference*]

Site Description: [*Brief description of period and nature of site*]

Dates/Ages:

			Lab. Ref.	Material	Archaeological Ref.
[*Type*] [*Type*]	[*Lab. abbrev.*]				
TL Context / Single Age	800 AD ± 50 (Dur87TLfg)		100-1/6	pottery	ABC-1a
	[*Overall error*]	[*Test year*] [*Technique*]	[*Sample ref.*]	[*Dated material*]	[*Context reference*]

— **TL Context Components:** [*Details of component TL dates/ages used to derive Context Date/Age*] ——

Archaeological Evidence: [*Excavator's brief description of context(s)*]

Site Director: [*Full name and institutional postal address*]

Reports: [*Details of excavation and laboratory reports*]

PART II

Section A. TL Measurements

1. **min.**([*mineral*]) **tech.**([*technique*]; [*grain size range, gsr*] μm)

Data tabulated for each sample:

2. **P** = [*value*] ± s.e. Gy 2a. **I/P** = [*value*] 3. **Slopes** [2nd/1st: [*value*] ± s.e.]
4. [*Type of plateau*] **Plateau** [± [*value*] %; [T_1 - T_2]]
4a. **Peak** [@ [*value*] °C ; [*heating rate*]°/s; [*pre-heat details if applicable*]]
5. **Stability**[[*interval*, T_1 - T_2]; [*period*]; [*storage T* °C]; [*result* ; [*value*] ± [*value*]%]]
6. *a* value = [*value*] , or *b* value = [*value*]

Section B. Dose-rate Measurements

Data tabulated for each sample:

1. **Total Effective Dose-rate** = [*value*] ± s.e. mGy/a [α = [*value*]% [*method*]; ß = [*value*]% [*method*]; γ = [*value*] % [*method*]; cos(mic) = [*value*] % [*method*]]
2. **Radon** [± [*value*] % [*method*]]
3. **Water** [Sample ([*value*] ± s.e. %); (Burial) Environment ([*value*] ± s.e. %)]

Section C. Error [[*Procedure : eA76 or specify other*]]

Section D. TL Age

Data tabulated for each sample:

TL Age[± [*random error*]; ± [*overall accuracy*]]

Special Remarks: [*Details of entries with * or any other additional information*]

KEY TO ABBREVIATIONS

STANDARD METHODS/TECHNIQUES/PROCEDURES

i	Inclusion	pd	Pre-dose	*a* Plat	Age plateau
fg	Fine-grain	MA	Multiple activation	*d* Plat	Dose plateau
mmi	Multi-mineral	ADD	Additive dose proc.	*s* Plat	TL Signal plateau
		Sb	Sensitivity baseline		
α-c	Alpha counting	FPh	Flame Photometry	TLD	TL dosimetry
AAS	Atomic absorption	NAA	Neutron Activation Analysis	XRF	X-ray fluorescence
β-c	Beta counting	PXE	PIXIE		
CAP	Capsule	SPEC	Spectrometer (SpEC = portable)		
Non-standard		AutoR	Auto regeneration	PTTL	Photo-transferred TL

MINERALS & ETC.

cal	Calcite	Nf	Sodium feldspar	*	Other
ft	Flint	p	Polymineral	-	Not applicable
f	Feldspar	q	Quartz	e	Equivalent to
Af	Unsep. alkali feldspar	z	Zircon		(used as prefix)
Kf	Potassium feldspar	por	Porcelain	a	Year

Terms: I, P, *a* , *b*, A, S_N, S_O, TAC: as defined in the literature.

Laboratory: Oxford **Entry:** 40

Site: Matupi Cave
Location: Zaire.
Grid Ref.: -
Site Description: The cave is located in the Mt. Hoyo limestone massif, in Ituri.

Dates			Lab. Ref.	Mat'l	Archaeological Reference
TL Single Ages:	24.7 ; ± 3.7 ka	(Ox87TLi)	200j3	hearth stone	ID115
	23.0 ; ± 3.5 ka	"	200j6	"	IJ120
	28.0 ; ± 3.0 ka	"	200j7	"	IA130-135
	33.4 ; ± 4.4 ka	"	200j17	"	IL140
	29.4 ; ± 3.0 ka	"	200j8	"	IA155
	70.0 ; ± 8.5 ka	"	200j9	"	IA195
	68.8 ; ± 8.8 ka	"	200j10	"	IB270
	80.0 ; ± 9.5 ka	"	200j12	"	IB380-400

Archaeological Evidence: The samples are from Late Stone Age levels, in decalcified loams, with Microlithic industry. The levels were overlain by Iron Age artefacts.

Site Director: Prof. F. Van Noten, Director of Museum of Art and History, Jubelpark 10, B1040 Brussels, Belgium.

Reports: Van Noten, F. (1977) Excavations at Maputi Cave. *Antiquity*, **LI**, 35-40.
Van Neer, W. (1984) Faunal remains from Matupi Cave, an Iron Age and Late Stone Age site in N.W. Zaire. *Academiae Analecta*, Klasse der Wetenschappen, 46(2), 59-76.

PART II
TECHNICAL SPECIFICATION

Section A. TL Measurements

1. Min(q) tech.(i ; 90 - 150 µm)

Sample Ref.	P ± s.e. (Gy)	I/P	Slps	s Plateau	Peak	Stability
200j6	43.1 ± 2.6	0	0.98 ± 0.05	± 6%; 325-400°	350°; 5°/s;-	-
200j7	68.5 ± 3.0	0	1.08 ± 0.05	± 3%; 350-450°	400°; 5°/s;-	
200j17	71.5 ± 3.5	0	1.30 ± 0.05	± 5%; 350-425°	400°; 5°/s;-	
200j8	50.6 ± 2.6	0	1.02 ± 0.05	± 5%; 350-400°	350°; 5°/s;-	
200j9	110.0 ± 6.0	0	1.09 ± 0.05	± 5%; 300-375°	325°; 5°/s;-	
200j10	122.5 ± 6.5	0	1.20 ± 0.05	± 3%; 300-350°	325°; 5°/s;-	
200j12	148.7 ± 7.7	0	0.98 ± 0.05	± 5%; 300-425°	325°; 5°/s;-	
200j3	38.5 ± 2.5	0	1.18 ± 0.05	± 6%; 325-400°	350°; 5°/s;-	

Section B. Dose-rate Measurements

Sample Ref.	Total Eff. Dose-rate	Dose-rate Components α	β	γ	cos.	Radon	Water Sample	Env.
	mGy/a	%	%	%	%	%	%	%
200j3	1.56 ± 0.23	-	13	82	5	0 ± 5	0 ± 2	20 ± 5
200j6	1.88 ± 0.28	-	28	68	4	"	"	"
200j7	2.45 ± 0.36	-	45	52	3	"	"	"
200j17	2.14 ± 0.32	-	37	60	3	"	"	"
200j8	1.72 ± 0.26	-	23	73	4	"	"	"
200j9	1.57 ± 0.24	-	25	72	3	"	"	"
200j10	1.78 ± 0.27	-	33	65	2	"	"	"
200j12	1.86 ± 0.28	-	34	64	2	"	"	"
Method			α-c FPh	SPEC	SpEC	α-c SPEC		

Section C. Error [cA76]

Section D. TL Age

Sample Ref.	TL Age ka	Errors Random ka	Overall ka.
200j3	24.7	-	3.7
200j6	23.0	-	3.5
200j7	28.0	-	3.0
200j17	33.4	-	4.4
200j8	29.4	-	3.0
200j9	70.0	-	8.5
200j10	68.8	-	8.8
200j12	80.0	-	9.5

Laboratory: Oxford **Entry:** 41

Site: Meer IV
Location: Near the Belgium-Dutch border, north of Antwerp.
Grid Ref.: -
Site Description: The site is located in the cover sands of the N. Campine. The industry belongs to the Late Upper Palaeolithic of N.W. Europe. It is characterized by a variety of projectile points, the most typical a blade with a curved back edge called the Tjonger point. The Tjonger site occupies the south east slope of the ridge and consists of an extended flint concentration,some associated with fireplaces.

Dates			Lab. Ref.	Mat'l	Archaeological Reference
TL Context Age:	11.8 ; ±1.2 ka	(Ox87TLfg)	255A	burnt flint	Tjonger site
Context Age Comps:	11.5 ; ± 1.2	-	255AI		Square I, E2, 44
	12.4 ; ± 1.6		255AII		Square II, D4, 111

Archaeological Evidence: The site belongs to the Epipalaeolithic complex of North-West Europe.

Site Director: Dr. F. Van Noten, Royal Museums for Art and History, Jubelpark 10, B1040 Brussels, Belgium.

Reports: Nijs, K. A Tjonger and a Mesolithic site at Meer, Belgium, in The "Big Puzzle" (Arts, M., Czlesla, Z. and Winter, D., Eds.). Proc. of the 1st. Int. Symp. on the subject of refitting stone artefacts. *BAR Int. Series*. Monrepos, 1988. (in press).

PART II
TECHNICAL SPECIFICATION

Section A. TL Measurements

1. Min(ft) tech.(fg ; 1 - 8 µm)

Sample Ref.	P ± s.e. (Gy)	I/P	Slps	s Plateau	Peak	Stability	a val
255AI	7.82 ± 0.4	0	-	± 2%; 275-350°	350°; 5°/s;-	275 - 350°; 0.5s; 18°; 100±3%	0.14
255AII	7.95 ± 0.4	0	-	± 2%; 325-375°	350°; 5°/s;-	325 - 375°; 0.5s; 18°; 100±3%	0.10

Section B. Dose-rate Measurements

Sample Ref.	Total Eff. Dose-rate	Dose-rate Components α	β	γ	cos.	Radon	Water Sample	Env.
	mGy/a	%	%	%	%	%	%	%
255AI	0.68 ± 0.08	25	20	35	20	0	0 ± 2	10 ± 2
255AII	0.64 ± 0.06	15	15	48	22	0	"	"
Method		α-c	α-c FPh	SPEC	SpEC	α-c SPEC		

Section C. Error [cA76]

Section D. TL Age

Sample Ref.	TL Age ka	Errors Random ka	Overall ka.
255AI [1]	11.5	-	1.2
255AII	12.4		1.6

Laboratory: Oxford **Entry:** 42

Site: Daylight Rock
Location: Caldey Island, Wales, UK.
Grid Ref.: SS 1497 9662
Site Description: An "open site" located on the present cliff top on the eastward extremity of Caldey Island, Dyfed.

Dates			Lab. Ref.	Mat'l	Archaeological Reference
TL Single Ages:	7.7 ; ±1.2 ka	(Ox89TLfg)	263f1	burnt flint	D3 level 39
	6.7 ; ±1.0 ka		263f2	"	F7 level 82
	7.9 ; ±1.2 ka		263f3	"	H1 level 37

Archaeological Evidence: The TL dates are significantly later than the A.M.S. dates (see below) from charred hazel nut shell from sealed contexts on the site. None of the samples was typologically diagnostic, and cannot be considered to have been in situ since their deposition.
C-14 dates (Accelerator Mass Spectrometer, Oxford University):
OxA2245: 9040 ± 90, OxA2246: 9030 ± 80 and OxA2247: 8850 ± 80 B.P.

Site Director: Andrew David, 7 Clifton Road, Isleworth, Middlesex, UK.

Reports: Lacaille, A. D. and Grimes,W. F. (1955) The Prehistory of Caldey. *Arch.Camb.*, 104, 85-165.
David, A. (1989) Some Aspects of the Human presence in W. Wales during the Mesolithic. In *The Mesolithic in Europe* (C. Bonsall Ed., Proc. 3rd. Int. Symp. of Mesolithic in Europe, 1985). Edinburgh.

PART II
TECHNICAL SPECIFICATION

Section A. TL Measurements

1. Min(ft) tech.(fg; 1 - 8 µm)

Sample Ref.	P ± s.e. (Gy)	I/P	SIps	s Plateau	Peak	Stability	a val
263f1	6.38 ± 0.38	0		± 3%; 350-425°	375°; 5°/s;-	350 - 425°; 0.5 a; 18°; 100 ± 3%	0.10
263f2	5.85 ± 0.35	0	-	± 3%; 300-400°	375°; 5°/s;-	300 - 400°; "	0.08
263f3	7.80 ± 0.40	0	-	± 3%; 300-375°	350°; 5°/s;-	300 - 375°; "	0.10

Section B. Dose-rate Measurements

Sample Ref.	Total Eff. Dose-rate	Dose-rate Components α	β	γ	cos.	Radon	Water Sample	Env.
	mGy/a	%	%	%	%	%	%	%
263f1	0.83 ± 0.08	8	11	64	17	0 ± 5	0 ± 2	15 ± 5
263f2	0.87 ± 0.09	14	16	53	17	"	"	"
263f3	0.98 ± 0.10	17	15	54	14	"	"	"
Method		α-c	α-c FPh	SPEC CAP	SpEC	α-c SPEC		

Section C. Error [eA76]

Section D. TL Age

Sample Ref.	TL Age ka	Errors Random ka	Overall ka
263f1	7.7		1.2
263f2	6.7	-	1.0
263f3	7.9	-	1.2

Laboratory: Oxford **Entry:** 43

Site: Yabroud,Shelter 1.
Location: Approximately 80 km. north of Damascus, Syria.
Grid Ref.: 33° 58' N, 36° 9' E.
Site Description: A major Middle/Early Palaeolithic shelter, discovered by A. Rust in 1930. Flints found in 1988 season in excavation of a broad burned area marked as a hearth zone in Shelter I, Rust's K2 area at ca.- 4.60m. depth.

Dates			Lab. Ref.	Mat'l	Archaeological Reference
TL Context Age:	195 ; ± 15 ka	(Ox90TLfg)	264c	burnt flint	Yabroud - 4.6m
Context Age Comps:	210 ; ± 20		264c1		1134
	185 ; ± 18		264c2		"
	192 ; ± 20		264c3		"
	205 ; ± 18		264c7		1133
	190 ; ± 18		264c11		"
	190 ; ± 16		264d2		1139

Archaeological Evidence: Associated cultural material (handaxes) relate to Rust's Kulturschicht, his Jungacheuleen, now Acheuleo-Yabrudian. The average date of 195 ka for this culture horizon is consistent with the TL dates from El Kowm, Hummal 1b (160 ka, J. Huxtable, Oxford.)

Site Director: Wm. Farrand, Dept. Geol. Sciences, Univ. Michigan, Ann Arbor, Mich.
Ralph Solecki, Dept. Anthrop.Columbia Univ, New York. 1988 season.

Reports:

Bordes, F. (1955) Le paléolithique inferieur et moyen de Jabrud (Syrie). *L'Anthropologie*, 59, 486-507.
Farrand, W. (1970) Geology, climate and chronology of Yabroud Rockshelter 1. In *Fundamenta* (Schwabedissen H., Ed.), 212 - 223.
Farrand,W. (1969) Chronology and palaeoenvironment of Levantine prehistoric sites as seen from sediment studies. *J. Arch. Sci.*, 6 , 369-392.
Heinzelin, J. de (1966) Revision du site de Yabroud. *Annales Arch. Arabes Syriennes*, XVI, 157-163.
Hennig, G. and Hours, F. (1982) Dates pour le passage entre l'Acheuleen et le Paleolithique moyen a El Kowm (Syrie). *Paléorient*, 8(1), 81-83.
Huxtable, J. (1988) TL dates on burnt flints from El Kowm. *Ancient TL* Date List Entry #22.
Rust, A. (1950) Die Höhlenfund von Jabrud. Syrien. Neumunster.
Solecki, R. S. (1970) A sketch of the Colombia Univ. arch. invest. at Yabroud. In (Schwabedissen, H., Ed.), *Fundamenta*, 199 - 201.
Solecki, R. S. and Solecki, R.L. (1966) New data from Yabroud. Preliminary report. *Annales Arch. Arabes Syriennes*, XVI, 121-154.
Solecki, R. S. and Solecki, R.L. (1986) A reappraisal of Rust's cultural stratigraphy of Yabroud Shelter I. *Paléorient*, 12(1), 53-59.

PART II
TECHNICAL SPECIFICATION

Section A. TL Measurements

1. Min(ft) tech.(fg ; 1 - 8 µm)

Sample Ref.	P ± s.e. (Gy)	I/P	SIps	s Plateau	Peak	Stability	a val
264c1	215 ± 15	0	-	± 5%; 350-425°	375°; 5°/s;-	350 - 425°; 0.5 a; 18°; 100 ± 3%	0.10
264c2	210 ± 15	0		± 5%; 325-375°	350°; 5°/s;-	325 - 375°; "	0.15
264c3	300 ± 15	0		± 3%; 325-375°	350°; 5°/s;-	325 - 375°; "	0.13
264c7	300 ± 15	0		± 3%; 325-375°	350°; 5°/s;-	325 - 375°; "	0.15
264c11	310 ± 15	0		± 5%; 300-425°	350°; 5°/s;-	300 - 425°; "	0.18
264d2	364 ± 24	0		± 5%; 350-425°	375°; 5°/s;-	350 - 425°; "	0.20

Section B. Dose-rate Measurements

Sample Ref.	Total Eff. Dose-rate	Dose-rate Components α	β	γ	cos.	Radon	Water Sample	Env.
	mGy/a	%	%	%	%	%	%	%
264c1	1.02 ± 0.20	25	25	38	12	0 ± 5	0 ± 2	9 ± 9
264c2	1.16 ± 0.23	35	22	33	10	"	"	"
264c3	1.61 ± 0.32	45	24	24	7	"	"	"
264c7	1.49 ± 0.30	44	22	26	8	"	"	"
264c11	1.65 ± 0.33	45	25	23	7	"	"	"
264d2	1.92 ± 0.39	60	20	14	6	"	"	"
Method		α-c	α-c FPb	SPEC	-	α-c SPEC		

Section C. Error [eA76]

Section D. TL Age

Sample Ref.	TL Age ka	Errors Random ka	Overall ka.
264c1	210	-	20
264c2	185		18
264c3	192		20
264c7	205	-	18
264c11	190	-	18
264d2	190		16

Laboratory: Oxford **Entry:** 44

Site: Port-Racine
Location: Cotentin Peninsula, France
Grid Ref.: x: 294,850 y: 232,337 Lambertian co-ordinates.

Site Description: A sea shore site at Saint-Germain des Vaux called Port-Racine. The occupation is at the foot of the cliffs and is attributable to the last interglacial. The occupation layer is Secteur 4 of the section by B. Van Vliet-Lanoe (1987). The stratigraphy is a little expanded and shows a layer of beach pebbles infiltrated by a gleyified loam(D2c), with lithic industry and associated hearths.

Dates			Lab. Ref.	Mat'l	Archaeological Reference
TL Context Age:	106 ; ± 10 ka	(Ox89TLfg)	265f	burnt flint	Secteur 4 of B.Van Vliet-Lanoe.
Context Age Comps.	109 ; ± 12		265f1		
	103 ; ± 12		265f2		

Archaeological Evidence: The gleyified loam (D2c) can be attributed to stage 5c of the Oxygen-isotope record by micromorphological studies.

Site Director: Mr. D. Cliquet, Conservateur au Musee d'Evreux, 6, Rue C. Corbeau, 2700 Evreux, France.

Reports: Fosse, G., Cliquet, D. and Vilgrain, G. (1986) Le Mousterien du Nord Cotentin. Actes du colloque int., Lille 4 - 6 Sept. 1984, 22nd C.P.F. *Suppl. au Bull. Assoc. pour Etude du Quat.*, 26, 141-155.

PART II
TECHNICAL SPECIFICATION

Section A. TL Measurements

1. Min(ft) tech.(fg; 1 - 8 µm)

Sample Ref.	P ± s.e. (Gy)	I/P	Slps	s Plateau	Peak	Stability	a val
265f1	190 ± 10	0	-	± 5%; 350-400°	375°; 5°/s; -	350 - 400°; 0.25 s; 18°; 100 ± 3%	0.1
265f2	133 ± 10	0	-	± 3%; 325-400°	375°; 5°/s;	325 - 400°; 0.25 s; 18°; 100 ± 3%	0.1

Section B. Dose-rate Measurements

Sample Ref.	Total Eff. Dose-rate	Dose-rate Components α	β	γ	cos.	Radon	Water Sample	Env.
	mGy/a	%	%	%	%	%	%	%
265f1	1.75 ± 0.26	22	18	53	7	0 ± 5	0 ± 2	20 ± 5
265f2	1.29 ± 0.19	9	11	71	9	"	"	"
Method		α-c	α-c FPh	SPEC	SpEC	α-c SPEC		

Section C. Error [eA76]

Section D. TL Age

Sample Ref.	TL Age ka	Errors Random ka	Overall ka
265f1	109		12
265f2	103	-	12

Laboratory: Oxford **Entry:** 45

Site: Trollesgave
Location: Zealand, Denmark
Grid Ref.: 55°17' N 11° 48' E.

Site Description: Small habitation site belonging to the Late Palaeolithic Bromme culture.

Dates			Lab. Ref.	Mat'l	Archaeological Reference
TL Single Ages:	11.7 ; ±1.4 ka	(Ox90TLfg)	601/31	burnt flint	99/103 :31
	11.1 ; ±1.2 ka	(Ox90TLfg)	601/32	"	99/103 :32
	12.0 ; ±1.4 ka	(Ox90TLfg)	601/145	"	99/103 :145

Archaeological Evidence: The TL dates were obtained from 3 flakes found in the central hearth of the habitation area. They belong to one and the same reduction sequence and are thus contemporary within a margin of a few minutes. Considering the error margin, the average TL date fits the already available C-14 dates of the refuse layer near the bottom of the adjacent lake deposits, which fix the age at approximately 11,100 b.p. plus a calibration factor of 500 to 1000 years.

Site Director: Anders Fischer, The Forest and Nature Agency, Slotsmarken 13, DK- 2970 Horsholm, Denmark.

Reports:

Fischer, A. and Mortensen, B.N. (1977) Trollesgave-bopladsen et eksempel pa anvendelse af EDB inden for arkaeologien. *Nationalmuseets Arbegdsmark*. 90 - 95. Copenhagen.

Fischer, A. and Mortensen, B. N. (1978) Report on the use of computers for the description and analysis of Palaeolithic and Mesolithic occupation areas.In *New Directions in Scandinavian Archaeology* (Kristiansen and Paludan-Muller Eds), 7- 22. Copenhagen.

Fischer A. An 11000 yr old school of flint knapping. Results from refitting the Late Palaeolithic site Trollesgave, Zealand, Denmark. *Acta Archaeologica*. Copenhagen. In press.

PART II
TECHNICAL SPECIFICATION

Section A. TL Measurements

1. Min(ft) tech.(fg; 1 - 8 µm)

Sample Ref.	P ± s.e. (Gy)	I/P	Slps	s Plateau	Peak	Stability	a val
601/31	10.45 ± 0.50	0		± 2%; 325-400°	375°; 5°/s;	325 - 400°; 0.25s; 18°; 100 ± 3%	0.10
601/32	9.85 ± 0.50	0	-	± 2%; 350-425°	375°; 5°/s;	350 - 425°; "	0.08
601/145	10.45 ± 0.50	0		± 5%; 325-425°	375°; 5°/s;	325 - 425°; "	0.08

Section B. Dose-rate Measurements

Sample Ref.	Total Eff. Dose-rate	Dose-rate Components α	β	γ	cos.	Radon	Water Sample	Env.
	mGy/a	%	%	%	%	%	%	%
601/31	0.89 ± 0.13	7	18	60	15	0 ± 5	0 ± 2	28 ± 7
601/32	0.89 ± 0.13	6	18	60	15	"	"	"
601/145	0.87 ± 0.13	8	15	62	15	"	"	"
Method		α-c	α-c FPh	SPEC	SpEC	α-c SPEC		

Section C. Error [eA76]

Section D. TL Age

Sample Ref.	TL Age ka	Errors Random ka	Overall ka.
601/31	11.7	-	1.4
601/32	11.1	-	1.2
601/145	12.0		1.4